NASA Technical Memorandum 107032

Compendium of Information for Interpreting the Microgravity Environment of the Orbiter Spacecraft

Richard DeLombard
Lewis Research Center
Cleveland, Ohio

August 1996

National Aeronautics and
Space Administration

CONTENTS

COMPENDIUM OF INFORMATION FOR INTERPRETING THE MICROGRAVITY ENVIRONMENT OF THE ORBITER SPACECRAFT

Richard DeLombard
National Aeronautics and Space Administration
Lewis Research Center
Cleveland, Ohio 44135

SUMMARY

Science experiments are routinely conducted on the NASA shuttle Orbiter vehicles. Primarily, these experiments are operated on such missions to take advantage of the microgravity (low-level acceleration) environment conditions during on-orbit operations.

Supporting accelerometer instruments are operated with the experiments to measure the microgravity acceleration environment in which the science experiments were operated. The Principal Investigator Microgravity Services (PIMS) Project at NASA Lewis Research Center interprets these microgravity acceleration data and prepares mission summary reports to aid the principal investigators of the scientific experiments in understanding the microgravity environment.

Much of the information about the Orbiter vehicle and the microgravity environment remains the same for each mission. Rather than repeat that information in each mission summary report, reference information is presented in this report to assist users in understanding the microgravity acceleration data.

The characteristics of the microgravity acceleration environment are first presented. The methods of measurement and common instruments used on Orbiter missions are described. The coordinate systems utilized in the Orbiter and accelerometers are described. Some of the Orbiter attitudes utilized in microgravity-related missions are illustrated. Methods of data processing are described and illustrated. The interpretation of the microgravity acceleration data is included with an explanation of common disturbance sources.

Instructions to access some of the acceleration data and a description of the Orbiter thrusters are explained in the appendixes. A microgravity environment bibliography is also included.

INTRODUCTION

NASA's Microgravity Science Program

The Microgravity Science and Applications Division (MSAD) of the NASA Headquarters Office of Life and Microgravity Sciences and Applications sponsors Principal Investigators (PI's) to fly science experiments in microgravity conditions on the NASA shuttle Orbiters, Russia's Mir space station, and the International Space Station. There are several Orbiter missions which have, as their primary payloads, laboratories containing many microgravity science experiments and are operated by the crew and/or by the PI's in ground control stations.

Many of the science experiments flown on the shuttle, and to be flown on the Mir and the International Space Station, require a knowledge of the microgravity environment for the analysis of the experimental data. The Microgravity Measurement and Analysis Project (MMAP) at NASA Lewis Research Center has responsibility for measuring the microgravity environment for the science experiment PI's and providing expertise in microgravity environment assessment.

This document presents information to assist the principal investigators in planning the acquisition and utilization of the microgravity environment data. This document includes a description of the microgravity environment, a brief description of microgravity acceleration measurement, types of common data processing techniques, and an overview of acceleration data analysis.

Acronyms and definitions used in this report are listed and defined in appendixes A and B, respectively.

What is Weightlessness?

On Earth, the force of gravity manifests itself by accelerating an object toward the Earth. A second object, such as a hand, a floor, or a table, which restrains the first object from falling exerts a force on the object which produces the sensation of an object's weight. It has been shown that, in the absence of air resistance, two articles will free-fall toward the Earth with the same acceleration rate, nominally 9.8 m/sec^2. There are no restraining forces on these articles during their free-fall, so they are weightless.

If enough horizontal velocity is imparted to a free-falling article, it can be made to orbit the Earth. To illustrate this, consider a hypothetical cannon on a mountain top (fig. 1). It is fired horizontally with 5 kg of gunpowder. The cannon ball falls to Earth 1 km from the cannon. The cannon is reloaded and fired with 10 km of gunpowder and the cannon ball falls to Earth 2 km away. The amount of gunpowder (in this hypothetical cannon) is increased until the cannon ball lands beyond the horizon. The cannon ball is starting to fall around the Earth. If more gunpowder is used, the cannon ball will fall beyond the horizon far enough as to not contact the Earth; it is then in orbit. Reference 1 provides a good background of gravity, microgravity, orbital flight, and microgravity sciences.

A major feature of an orbiting spacecraft is the apparent lack of gravity that is due to the free-fall condition of orbit. On a spacecraft in orbit, any freely floating particle has no weight because there are no restraining forces imparted to it and the particle is in free-fall like the spacecraft. For any free-floating particle not colocated with the spacecraft center of mass, the particle is in a different orbit than the spacecraft and has a relative acceleration with respect to the spacecraft. This relative acceleration situation is disturbed by other acceleration effects which are present in a spacecraft, such as aerodynamic drag, spacecraft motion, rotating machinery, transient equipment, and crew actions.

Weightlessness is a nebulous term in this situation because there are accelerations involved in the spacecraft environment. The term microgravity has become the common descriptive term for the low-level acceleration and vibration environment experienced onboard the spacecraft during orbital flight.

ACCELERATION ENVIRONMENT

The on-orbit acceleration environment is classified into three major categories of disturbances: quasi-steady, oscillatory, and transient.

Acceleration Categories

Quasi-Steady Accelerations.—Quasi-steady accelerations are those that vary little over long periods of time, typically with periods longer than a minute. These are also referred to as residual accelerations. The major contributors to the quasi-steady acceleration environment are aerodynamic drag, gravity-gradient effects, and Orbiter rotational accelerations. Aerodynamic drag effects are primarily functions of the Orbiter attitude, the Orbiter altitude, and the atmospheric density. For most microgravity science missions, the Orbiter attitude is determined by the integrated science requirements of the primary payload(s). Atmospheric density varies with the 11-yr solar cycle, Orbiter altitude, time of year, and position within an orbit. Gravity-gradient accelerations result from an object being displaced from the flight path of the vehicle center of mass. Rotational accelerations acting on a body within the Orbiter are comprised of radial and tangential accelerations (from vehicle rotational motion). For a description of quasi-steady accelerations in an orbiting spacecraft, see reference 2.

Oscillatory Accelerations.—Oscillatory accelerations are those that are harmonic and periodic in nature with a characteristic frequency. Characteristic frequencies on orbiting space laboratories are in the sub-Hertz to hundreds of Hertz range. Typical examples of oscillatory disturbances are rotating or reciprocating pumps, communication antenna dither motion, and Orbiter structural oscillation. A standard Orbiter refrigerator/freezer has a pump which causes vibrations at 22 Hz. The Orbiter Ku-band antenna has a strong 17-Hz dither which is evident during most of a mission when this antenna is utilized. There are several Orbiter structural modes in the 1- to 10-Hz frequency regime which are often excited by transient acceleration events or by other oscillatory accelerations. These structural mode frequencies vary slightly among the different Orbiter vehicles and payloads.

Transient Accelerations.—Transient accelerations are those that are nonperiodic in nature and typically have a duration of less than 1 sec. The energy in the disturbance is typically spread across the frequency range from the sub-Hertz to hundreds of Hertz range. These broad-band disturbances may excite oscillations of the Orbiter, experiment carrier, subsystems, or experiment structural modes. There are several Orbiter structural modes in the 1- to 10-Hz region which are typically excited by transient disturbances.

Common sources of transient disturbances are Orbiter thruster operations, some Orbiter Remote Manipulator System (RMS) operations, satellite launches, and some crew actions. Some of these sources may be inhibited or controlled to minimize the impact on microgravity science experiments.

Vehicle Response

The Orbiter vibrational response to the previously described acceleration environment is extremely complex and, in general, difficult to characterize by a single measurement, taken over a single discrete period of time, at a single location. The various disturbance sources described previously do not occur simultaneously but instead occur in a random fashion. Furthermore, there are multiple structural paths between the disturbances at any one time and the location of a particular microgravity experiment. The acceleration inputs to an experiment and its vibratory response constitute a highly complex multiple-source, multiple-path dynamic system.

The quasi-steady accelerations at frequencies below the vehicle's structural mode frequencies are experienced throughout the vehicle because the vehicle is a rigid body in this frequency range. The magnitude of some quasi-steady accelerations (generated by Orbiter rotational motions, for example) are dependent on the location within the vehicle and the motion of the vehicle.

The accelerations at frequencies higher than the vehicle's lowest structural mode frequency, though, have a very localized magnitude and direction. The propagation of oscillatory accelerations throughout the vehicle and payload is dependent on the characteristics of the structural path through which the accelerations are transmitted. These characteristics may change based on changes in the vehicle and payload configuration such as those that occur after a satellite is launched.

Transient accelerations quite often cause vehicle vibrations to occur across a wide-frequency band. This will also cause a "ringing" effect of the vehicle structure at the primary structural frequencies.

The acceleration inputs to an experiment, consequently, constitute a highly complex multiple-source, multiple-path dynamic system.

MEASUREMENT

Acceleration Sensors

Many acceleration sensors, which are commonly used for microgravity acceleration measurements, are designed to measure the acceleration of the sensor case (or mounting structure) relative to inertial space for navigation purposes. These sensors include pendulous mass sensors (fig. 2) and electrostatically suspended sensors (fig. 3). Pendulous mass sensors use an internal proof mass on a cantilever to sense the acceleration of the sensor case relative to inertial space. The electrostatically suspended proof mass sensor utilizes electrostatic forces to center a proof mass in a chamber. In either sensor, the position of the mass is detected and a restoring force (either magnetic or electrostatic) is applied to keep the mass centered. The output acceleration signal is then derived from the restoring force signal.

Other types of acceleration sensors measure the movement of an inertial mass relative to the sensor case, such as a ball in a viscous fluid (fig. 4). The polarity of this type of sensor depends on the relative densities of the inertial mass and the fluid (fig. 5). This type of sensor is referred to here as a "fluidic suspended sensor." In these sensors, the movement of the inertial mass (the ball) is interpreted to indicate the acceleration of inertial space relative to the sensor structure.

The polarity of a sensor (as reflected in the data) needs to be considered when analyzing any acceleration data, particularly in the quasi-steady acceleration regime. The frame of reference also needs to be considered in the process of correlating acceleration data with science results.

Frame of Reference

An experiment chamber (as part of an experiment which is operated on the Orbiter) is exposed to an acceleration environment caused by the vehicle, the crew, other experiments, and the experiment apparatus itself. Ideally, the experiment chamber would free-float in inertial space to be totally free of outside acceleration disturbances.

In general, an experiment chamber is composed of a portion fixed to the vehicle (e.g., fluid chamber walls, crystal growth ampoule) and a portion which is "free-floating" from the vehicle (e.g., bubble in fluid, molten liquid bridge).

The acceleration disturbances coming from the vehicle have a direct effect on the fixed portion which causes a relative effect to the free-floating portion. As an illustration, a trace particle in a liquid (fig. 6) is not moving within a fluid. With an impulsive acceleration disturbance (e.g., thruster firing) in the +X direction, the Orbiter and fixed chamber walls move in the –X direction. Relative to the Orbiter and fixed chamber walls, the particle is subject to an acceleration in the +X direction. Because this acceleration is imparted to the Orbiter vehicle in the reverse direction by a forward-facing thruster, the vehicle body goes in the –X direction. This would be interpreted as a negative acceleration by a pendulous mass sensor or an electrostatically suspended sensor, but a fluidic suspended sensor would interpret this as a positive acceleration.

A scientist typically utilizes the acceleration relative to a frame of reference fixed to the chamber wall or structure. The reported accelerations are those experienced by the free-floating experiment material (e.g., molten liquid bridge, flame body, or trace particles).

Some acceleration measurement systems measure the accelerations of the mounting surface to which the triaxial sensor head is mounted, relative to inertial space. The axis polarity must be reversed for application to experiment-based observations of free-floating articles.

On the other hand, the polarity of a fluidic suspended sensor (with the proof mass density higher than that of the fluid) would be the same as the experiment-based observations. The Passive Accelerometer System (PAS) utilizes a steel ball within a column filled with a buffered water solution to sense and display the low-frequency accelerations.

Accelerometer Systems

There are various accelerometer systems available for measuring the microgravity conditions during experiment operations on orbit. The salient features of some of these accelerometer systems are summarized here and the missions flown by each system are shown in table I.

Fluid Experiment System (FES) Accelerometer.—The FES accelerometer measures acceleration at the base of the rack in which the FES apparatus is mounted. The accelerometer is a three-axis device utilizing an electrostatic suspended proofmass sensor. A low-pass filter set for 50 Hz is applied to the data. Data are analyzed and reported in reference 3.

The FES accelerometer was developed by Bell Aerospace under contract to NASA Marshall Space Flight Center (MSFC).

High Resolution Accelerometer Package (HiRAP).—The HiRAP is a three-axis accelerometer utilizing pendulous accelerometer sensors. The data are passed through a 20-Hz low-pass filter prior to be digitized.

The HiRAP instrument was developed by KMS Fusion, Incorporated which was under contract to NASA Johnson Space Center (JSC) to acquire data for shuttle aerodynamic research.

Honeywell In-Space Accelerometer (HISA).—The HISA is a three-axis accelerometer utilizing pendulous accelerometer sensors. The data are passed through a 19.5 Hz low-pass filter prior to being digitized. The dc bias is electronically eliminated resulting in frequency response from 0.025 to 19.5 Hz.

The HISA was developed by Honeywell Incorporated to monitor oscillatory and transient accelerations onboard the spacecraft. Further technical details on the operation of the HISA can be found in references 4 and 5.

Microgravity Measurement Assembly (MMA).—This general purpose accelerometer was developed to measure the microgravity environment to support microgravity experiments in the Spacelab module. Data are available in near-real-time (NRT) in the Payload Operations Control Center (POCC) or other operations control centers during a mission. The MMA utilizes pendulous mass sensors. An electrostatic suspended sensor is under development for future use by MMA.

The MMA unit was developed by the European Space Research and Technology Center in The Netherlands.

Microgravity Measuring Device (MMD).—The Microgravity Measuring Device was developed to characterize the microgravity environment of the Wake Shield Facility (WSF) free flyer and the WSF carrier. The MMD was sponsored by the Space Vacuum Epitaxy Center of the University of Houston in support of the JSC. Data are recorded at 25 samples/sec for each of three axes. Data are downlinked to the JSC control center during a mission. The MMD utilizes pendulous proofmass sensors.

The MMD was subsequently used in the Orbiter middeck in support of crew exercise disturbance studies by JSC. The MMD unit was developed by JSC.

Orbital Acceleration Research Experiment (OARE).—The OARE is a three-axis accelerometer utilizing an electrostatically suspended proofmass sensor which measures low-frequency (lower than 0.1 Hz) accelerations of the Orbiter vehicle. The OARE instrument is mounted on the cargo bay floor, very close to the center of mass of the vehicle. Raw data are recorded on the payload tape recorder and downlinked. The data are also processed with a trimmed mean filter and recorded on OARE internal memory for access after the mission. Compensated data are available on a file server after the mission.

The OARE instrument was developed by KMS Fusion, Incorporated (currently Canopus Systems, Inc.) under contract to JSC to acquire data for shuttle aerodynamic research. The OARE instrument is presently managed by LeRC and is currently used to support microgravity science experiments.

Passive Accelerometer System (PAS).—The PAS was developed at the Center for Microgravity and Materials Research at the University of Alabama in Huntsville (UAH) to estimate the magnitude of quasi-steady accelerations related to atmospheric drag and gravity-gradient effects (ref. 6). PAS operations are based on a simple method used to measure viscosity. The instrument is composed of a steel spherical mass in a tube filled with a buffered water solution. The time it takes the mass to drift along a known distance in the fluid is used to calculate the velocity of the mass, and from that the acceleration is calculated.

Quasi-Steady Acceleration Measurement (QSAM) System.—The QSAM system measures the quasi-steady and vibration-acceleration environment experienced in the Spacelab module. The QSAM instrument has dual two-axis invertible sensors for low-frequency acceleration measurements and a triaxial sensor head (TSH) for high-frequency measurements. The QSAM utilizes pendulous proofmass sensors.

The QSAM unit was developed by Deutsche Forschungsanstalt fur Luft und Raumfahrt (DLR) in Germany.

Space Acceleration Measurement System (SAMS).—A SAMS unit measures acceleration at up to three experiment locations simultaneously and records the raw data in digital format on optical disks. The SAMS units were developed by LeRC for use in multiple locations on the Orbiter in support of multiple microgravity missions. There are two configurations of SAMS units, one for the Orbiter middeck, Spacelab module or SPACEHAB module and one for the Spacelab MPESS carrier in the Orbiter cargo bay. For SAMS units mounted on the Spacelab MPESS experiment carriers, some of the data are downlinked to the POCC for access in near-real-time by PI's. The SAMS TSH's heads utilize pendulous proofmass sensors.

After the mission, the recorded data are processed to result in engineering units. CD-ROM's are then produced containing these data for distribution to users. The downlink data are processed in NRT in the POCC for display and analysis during the mission and are also distributed via CD-ROM. The processed data are also available from an Internet-connected file server.

The SAMS units are managed by LeRC. One SAMS unit has also been installed on the Russian Mir Space Station. Further information on SAMS may be found in the literature (refs. 7 to 9).

Three-Dimensional Microgravity Accelerometer (3DMA).—The 3DMA includes three remote TSH's and three single-axis invertible sensors for on-orbit measurement of low-frequency accelerations. The 3DMA utilizes pendulous proofmass sensors. All of the data are recorded on the 3DMA instrument, and some of the data may be downlinked to the POCC during a mission.

The 3DMA was developed at the Center for Materials Development in Space at UAH.

COORDINATE SYSTEMS

There are several coordinate systems which need to be considered when analyzing acceleration data. Care must be exercised when dealing with data (whether acceleration environment, Orbiter operations, or experimental data) to refer to the proper coordinate system.

Orbiter Center of Mass (CM) (On Orbit)

The Orbiter vehicle center of mass is generally controlled to be within a small volume with the largest dimension being 0.8 m in the Orbiter structural X-axis direction. Structural coordinate system dimensions for a typical location of the CM are given in table II.

Orbiter Body Coordinate System

The body coordinate system of the Orbiter is illustrated in figure 7. The Orbiter body coordinate system (X_b, Y_b, Z_b) is defined as a right-handed, orthogonal coordinate system with the $+X_b$ axis extending forward (through the Orbiter nose) and the $+Z_b$ axis extending downward through the Orbiter belly. The $+Y_b$ axis completes the right-handed system and extends to starboard (ref. 10). The origin of this coordinate system is located at the CM of the vehicle.

Orbiter operational data, such as attitude rates, are typically given in the Orbiter body coordinate system.

Orbiter Structural Coordinate System

The structural coordinate system (X_o, Y_o, Z_o) of the Orbiter is illustrated in figure 8. The Orbiter structural coordinate system is defined as a right-handed, orthogonal coordinate system with the $+X_o$ axis extending aft (through the Orbiter tail) and the $+Z_o$ axis extending upward out of the Orbiter payload bay. The $+Y_o$ axis extends to starboard (ref. 11). The origin of this coordinate system is at the tip of the shuttle external fuel tank.

The physical location of equipment within the Orbiter is usually specified in terms of this system.

Orbit Local Vertical/Local Horizontal Coordinate System

The orbit local vertical (LV)/local horizontal (LH) coordinate system (X_{LVLH}, Y_{LVLH}, Z_{LVLH}) is illustrated in figure 9. This coordinate system is based on the Orbiter direction of motion and the center of the Earth. It is independent of the vehicle's attitude. The $+X_{LVLH}$ axis (LH direction) is in the orbital plane and colinear to the Orbiter velocity vector (VV). The $+Z_{LVLH}$ axis (LV direction) is toward the center of the Earth. The $+Y_{LVLH}$ axis completes the right-handed coordinate system. The origin of this coordinate system is the vehicle CM (ref. 12).

The Orbiter orbital attitude is quite often given in reference to LV and the velocity vector (LH) (see the section Orbiter Attitudes).

Sensor Head Coordinate System

Another axis system is that of the accelerometer sensor head. Sensor heads may be of one, two, or three axes with an inherent orthogonal axis system. The SAMS TSH coordinate system is shown as an example in figure 10. This sensor head coordinate system is related to a shuttle coordinate system by the orientation of the sensor head as mounted to the shuttle. In applying the acceleration data to an experiment, the relationship of the sensor head polarity and orientation relative to the experiment chamber must be determined.

Coordinate Systems Conversion

Sensor Head Location.—To convert a sensor head location from the structural coordinate system to the body coordinate system, the following method is used.

The vehicle center of gravity (CG) location in structural coordinates is (X_{OCG}, Y_{OCG}, Z_{OCG}). The location of a sensor head in structural coordinates is (X_{OSH}, Y_{OSH}, Z_{OSH}). The position vector from the CG to the sensor head in structural coordinates is given by

$$(X_{OBSH}, Y_{OBSH}, Z_{OBSH}) = (X_{OSH} - X_{OCG}, Y_{OSH} - Y_{OCG}, Z_{OSH} - Z_{OCG})$$

Because $X_{Body} = -X_{Structural}$ (i.e., $X_B = -X_O$), $Y_B = Y_O$, and $Z_B = -Z_O$, and because the body coordinate system's origin lies at the CG, the location of the sensor head in body coordinates is given by

$$(X_{BSH}, Y_{BSH}, Z_{BSH}) = (-X_{OBSH}, Y_{OBSH}, -Z_{OBSH})$$

This conversion method can be used for any object of known location in the Orbiter.

Sensor Head Orientation.—Conversion of acceleration data from one axis system to another, such as from Orbiter structural axes to experiment-based axes, requires the knowledge of the relative orientations of the two axis systems. Given the parameters in table III where $\lambda_{u'u} = \cos \Phi$, for Φ the angle between the u′-axis and the u-axis, the equations for a simple rotation transformation are

$$\begin{aligned} x' &= \lambda_{x'x}x + \lambda_{x'y}y + \lambda_{x'z}z \\ y' &= \lambda_{y'x}x + \lambda_{y'y}y + \lambda_{y'z}z \\ z' &= \lambda_{z'x}x + \lambda_{z'y}y + \lambda_{z'z}z \end{aligned}$$

Orbiter Attitudes

The Orbiter is flown in attitudes determined by the requirements of the payload(s) being flown. Some attitudes are based on a need for a specific orientation of the payload bay relative to the Earth, the Sun, or some other point in inertial space. Some attitudes are based on operational constraints such as minimal number of thruster firings or specific orientation of the quasi-steady acceleration vector.

The attitudes selected for a mission are quite often a compromise among the requirements of the various payloads and the attitude changes during a mission based on the requirements of the active payloads.

The typical Earth-oriented attitudes are illustrated in figure 11. The attitude names are based on the Orbiter body axis orientation relative to local vertical and the velocity vector (ref. 12). The attitude at the upper left is referred to as –ZLV/–XVV which indicates that the Orbiter –Z body axis is toward the Earth (local vertical) and –X body axis is in the direction of flight (velocity vector).

The Orbiter attitude determines major features of the microgravity environment due to the frequency and intensity of the required thruster firings, rotational effects, atmospheric drag and the resultant magnitude, and the direction of the quasi-steady residual acceleration vector at the experiment site within the vehicle.

DATA PROCESSING

Data Processes

Various methods may be applied to the sampled data set produced by accelerometer systems. The method or methods applied to the data are determined by the nature of information desired from the analysis. Common processes applied to acceleration data are described here with the basic information which is typically extracted from each method.

Vector Versus Single Axes.—In some cases, an experiment may be interested in acceleration data from individual axes. There may be a high degree of symmetry in the experimental apparatus that makes a single axis acceleration predominate in its effect on the science apparatus.

The common method of processing to be applied to multidimensional (either two or three axes) accelerometer data is to combine the individual orthogonal axis data into a vector magnitude. The vector magnitude of an individual data point is derived by the following equation:

$$\left|V_j\right| = \sqrt{\left(X_j^2 + Y_j^2 + Z_j^2\right)}$$

Acceleration Versus Time.—This data plot illustrated in figure 12 plots the acceleration data points as acquired in time. Individual axis data, vector magnitude, or statistical representations may be chosen.

A peak acceleration function displays the peak acceleration in successive intervals of time. An average acceleration function displays the average acceleration in successive intervals of time.

Arithmetic Mean and Root-Mean-Square (rms) Versus Time.—By choosing a small interval of time relative to the sampling rate and the total time of the acceleration data, several processes (such as an arithmetic mean and rms) may be applied to each interval. Typically, this interval can range from tens of seconds to minutes, depending on the sample rate of the data and/or the needs of the PI.

Arithmetic Mean Calculation: Applying an arithmetic mean to the data within the interval results in a total set of data with a frequency response less than the inverse of the time interval. An average plot may be produced by calculating an interval average of each axis and then combining the results into a vector magnitude representation.

Root Mean Square (rms) Calculation: By applying an rms calculation to the interval of data, information relative to the periodic content of the data is apparent. A rms plot may be produced by calculating the rms of an interval of data for each axis and then combining the results into a vector magnitude representation.

Acceleration Power Spectral Density Versus Frequency.—This data plot, illustrated in figure 13, plots the acceleration power spectral density (PSD) against frequency. This data plot may use vector magnitude or individual axis data.

Applying a fast-Fourier-transform (FFT) routine to a window of data transforms the time-sampled data into the frequency domain. The data in figure 13 is the same as that in figure 12. The obvious oscillation occurring with a period of about 3 sec in figure 12 appears as the peak at 0.3 Hz in figure 13.

The power spectral density illustrates where the energy content of the total vibration resides. This is useful for examining the data for its effects on specific experiments.

Acceleration Power Spectral Density Versus Time Versus Frequency.—Calculating successive acceleration power spectral density and appending them in time results in a three-dimensional plot of the acceleration data (fig. 14).

Activities which contain distinct frequencies are apparent by horizontal bands or bars in the plot. The vehicle vibration modes are in the range between 3 and 10 Hz, the Ku-band antenna operates at 17 Hz and a refrigerator/freezer compressor operates at 22 Hz. Short time-based events (such as a thruster firing) are manifested by narrow vertical lines.

This type of data plot allows several types of information to be extracted. Some experiments are sensitive to vibrations in a certain frequency region, whereas others are sensitive to impulsive types of disturbances with energy spread across the entire frequency spectrum.

Data Access

Access to acceleration data is desired as soon as possible during or after experiment operations. In some cases, knowledge of the acceleration environment is needed in preparation for future experiment operations.

Most accelerometer systems record data by means of magnetic tape storage, optical disk storage, or magnetic hard disk. The data are returned to Earth, processed into engineering units, and then made available for analysis. The time delay for this may range from days to months after the experiment operations. Final data products are available in a variety of formats ranging from survey reports describing the mission to acceleration data in engineering units on floppy disks, CD-ROM's, and network accessible files.

In some accelerometer systems, data are available in NRT during the mission for conversion to engineering units and availability for analysis.

For accelerometer systems with downlinked data available in the POCC, standard processes and data display techniques are utilized. In some cases, the raw data are also available for experiment teams to process and analyze directly on their ground support equipment.

SAMS and OARE acceleration data are available on a file server for access over the Internet. The files are primarily for PI's funded by MSAD but other organizations with a demonstrated need may also access the data. In the future, it is planned that the mission summary reports will also be available over the Internet. The file server Internet name is `beech.lerc.nasa.gov` and the data are in a directory entitled pub. Appendix C—Accessing SAMS Data Files Via Internet contains further instructions on utilizing this file server.

For questions about access to this data, contact

Richard DeLombard
PIMS Project Manager
e-mail: pims@lerc.nasa.gov
Telephone: 216–433–5285
Facsimile: 216–433–8660

Standard Services

Standard reports are prepared after each MSAD science mission with an accelerometer system. The reports describe the accelerometer systems flown on the mission and summarize the data acquired by the SAMS and OARE accelerometer systems. Other accelerometer systems are summarized when they have been used to support MSAD PI's. Reports which have been prepared for previous missions are listed in the bibliography.

For the SAMS data acquired from missions, CD-ROM's are prepared and are available for distribution. For the SAMS and OARE data acquired from missions, the processed data is available on an Internet-connected file server for access by users.

Specialized data processing is also available for MSAD-sponsored PI's.

DATA INTERPRETATION

Acceleration Events Characteristics

Many events onboard the shuttle may be characterized by their acceleration signature. Whereas each occurrence is essentially unique, there are distinguishing patterns for similar types of events. The following sections are a summary of what is currently known about these types of events. The characterization will continue to be refined in the future.

Thrusters.—There are three basic types of thrusters on the Orbiter which are used during on-orbit operations (see Appendix D—RCS and OMS Engines Description). Vernier Reaction Control System (VRCS) thrusters, which provide about 24 lb of thrust, are used for fine attitude control. A thruster of this type will cause a disturbance at or below 10^{-4} g.

Primary Reaction Control System (PRCS) thrusters, which provide about 870 lb of thrust, are used for attitude changes. A thruster of this type will cause a disturbance at or below 10^{-2} g.

Orbital Maneuvering System (OMS) thrusters, which provide about 6,000 lb of thrust, are used for orbit insertion, orbit changes and de-orbit. The OMS are not typically used during Spacelab module operations.

These three thruster types have similar signatures (figs. 15, 16, and 17), but are differentiated by acceleration magnitude and duration. The stars in figures 15 and 16 indicate the time that thrusters were fired. The vernier and primary thrusters are typically fired for a very short event (typically 80 msec to 1 sec). The OMS thrusters operations can occur from seconds to minutes in length.

A thruster action is an impulse action and contributes energy across a wide frequency band. Figure 18 (see color plate 1) illustrates four thruster events which occurred in a 1 min time frame on STS–62 and were approximately 15 sec apart. The coarseness of the data plot is due to the short time interval included in the plot. These same thrusters are shown in figure 16, starting at 150 sec.

Crew Exercise.—Disturbances from crew exercise are dependent on the type of exercise device utilized, the particular crew member's physical characteristics, and the robustness of the exercise. The method (if any) of vibration isolation or control incorporated in the exercise device has a direct effect on the microgravity environment. Experimental investigations are ongoing to find the optimal method of crew exercise and vibration isolation for the devices. Exercise remains necessary for the health and well-being of the crew members.

The disturbance from a treadmill shown in figure 19 typifies crew exercise-induced disturbances. The basic frequency of 2.3 Hz originates with the foot fall frequency of the crew member. One-half of that frequency is the stride rate with the disturbance caused by the side-to-side motion of the crew member's body. With a fundamental

vibration mode of the Orbiter at 4.7 Hz, a significant amount of acceleration is observed at this frequency. The crew exercise activities usually last for 20 to 30 min for each crew member daily during a mission.

Disturbances caused by crew exercise on a bicycle ergometer are similar in nature.

Life Science Experiments.—Some life sciences experiments employ devices such as rotating chairs for crew members and centrifuges for plants and animals. The data shown in figures 12 and 13 were acquired during an experiment in which one crew member was seated in a chair while another crew member manually rotated the chair. The chair rotation rate was approximately one revolution every 3 sec.

Shuttle Maneuvers.—Maneuvers to change the shuttle attitude can be significant sources of disturbance. During a typical mission, attitude maneuvers may be performed for a variety of reasons, such as navigation, communications, and Orbiter thermal requirements. The disturbances created are a combination of thruster firing disturbances (described in the previous section) together with rotational and translational accelerations as the vehicle is reoriented.

The quasi-steady acceleration level changes between attitudes is illustrated in figure 20 from OARE data on STS–62. The Orbiter was reoriented from the –XLV/–ZVV attitude to the –XLV/+ZVV attitude. The Z-axis acceleration can be seen to change sign since the Orbiter reversed direction in the Z-axis. The high-level acceleration which occurred during the maneuver is due to the rotational and translational accelerations during the maneuvers.

Shuttle Equipment.—Some equipment on the shuttle, such as the Ku-band antenna and refrigerators, operate almost continuously during on-orbit operations.

The Ku-band antenna has a 17-Hz dither frequency for the pointing control system. This signature (figs. 14, 18, 21, and 22) is quite often found in the acceleration environment of the Orbiter and can be quite significant compared with the background environment.

Notice the relative strengths of the first and second harmonics of this disturbance at 34 and 51 Hz. Note that the data in figure 22 were acquired during a crew sleep period and were filtered by the SAMS instrument with an eight pole filter at 25 Hz.

The refrigerators commonly used in the Spacelab module and in the Orbiter middeck have a characteristic frequency of 22 Hz and harmonics (figs. 13 and 14) and a typical cycle time of 3 min on and 9 min off. A different refrigerator used in the SPACEHAB module on the SH–2 mission operates with a frequency of 60 Hz.

Other Orbiter equipment, which does not contribute significantly to microgravity disturbances, has been investigated. The movements of the cargo bay cameras and the Ku-band antenna (apart from the dither mentioned earlier) do not appear to significantly affect the environment.

Atmospheric Drag.—The shuttle experiences atmospheric drag due to the slight atmosphere which exists at orbital altitudes. The magnitude of this atmospheric drag depends on many variables, such as altitude, attitude, orbital inclination, time of year, day/night portion of the orbit, etc. Atmospheric drag is characterized by its variation with an orbital period (typically 90 min). The orientation of the drag is opposite the velocity vector.

The variation in the quasi-steady acceleration in the Z_b-axis of the shuttle in a –XLV/–ZVV attitude during STS–62 is shown in figure 23. During this time, the shuttle was in a near-circular orbit with an altitude which varied between 161 and 163 n mi.

The variation in the quasi-steady acceleration in the Y_b axis of the shuttle in a –ZLV/+YVV attitude during STS–62 is shown in figure 24. In this figure, this attitude was maintained from hour 320 into hour 328. During this time, the shuttle was in an elliptical orbit with apogee and perigee altitudes of 138 and 105 n mi, respectively. This difference in altitudes accentuated the variation in drag accelerations compared to those occurring in a more circular orbit. This is due to the difference in atmospheric density experienced at the different altitudes during one orbit. In this attitude, the majority of the drag is aligned with the Orbiter Y_b-axis since that axis is in the direction of flight.

Vehicle Location.—There are variations in the quasi-steady acceleration levels depending on the location within an orbital vehicle. These variations are due to the effects of the gravity gradient and rotational accelerations (see the section Quasi-Steady Accelerations and ref. 13). Figures 25 and 26 illustrate the difference between OARE data as acquired at the OARE location (fig. 25) and at an experiment location (fig. 26) almost 5 m away.

Satellite Launches.—Some MSAD science experiment payloads are manifested on missions which include satellite launches from the cargo bay of the shuttle. One such mission, the USMP–1 on STS–52, included the launch of the LAGEOS satellite on the first day of the mission. This event is shown in figure 27 and is characterized by the shuttle maneuvers prior to and after the launch and the short discrete high-level disturbance when the satellite was actually launched.

CONCLUDING REMARKS

The microgravity acceleration environment is typically measured during microgravity science missions on the Orbiter. These acceleration data are processed and presented to the scientists to aid in the analysis of their scientific data.

This document includes information which is common to different missions and complements the contents of the Mission Summary Reports produced by the PIMS Project at NASA LeRC. It is anticipated that this compendium of information will be expanded in the future when additional information is available.

With the information in this document, scientists will be better able to apply the acceleration data to their scientific data.

ACKNOWLEDGMENTS

The author wishes to thank several people for their contributions to this report. The data were extracted from work done by four members of the PI Microgravity Services project at NASA LeRC. Melissa J.B. Rogers, Kim Destro-Sidik, Ken Hrovat, and Doug Deutsch, all employees of Tal-Cut Company, have spent many hours deciphering and interpreting the acceleration environment data. Brian Matisak, Teledyne Brown Engineering, Huntsville, Alabama has spent many hours reviewing and explaining the orbital aspects of the acceleration environment for the author.

TABLE I.—ACCELEROMETER SYSTEMS BY FLIGHT

Mission	Microgravity payload	Launch	FES	HiRAP	HISA	MMA	MMD	OARE	PAS	QSAM	SAMS	3DMA
STS–6, 7, 8, 9, 11, 13, 24, 26, 30, 35				X								
STS–17 (51–B)	Spacelab 3	4/85	X									
STS–32		1/90		X	X							
STS–40	SLS-1	6/91		X				X			X	
STS–43		8/91									X	
STS–42	IML-1	1/92	X								X	
STS–50	USML-1	6/92		X				X	X		X	
STS–47	SL-J	9/92									X	
STS–52	USMP-1	10/92		X							X	
STS–55	SL-D2	4/93		X		X						
STS–57	SH-1	6/93									X	X
STS–58	SLS-2	10/93		X				X				
STS–60	SH-2	2/94					X		X		X	X
STS–62	USMP-2	3/94		X				X	X		X	
STS–65	IML-2	7/94		X			X	X		X	X	
STS–66	PCG	11/94									X	
STS–63	SH-3	2/95									X	X

TABLE II.—ORBITER CENTER OF MASS (CM) LOCATION (TYPICAL)

Orbiter structural axis	Orbiter structural location, in.
X	1096
Y	0.38
Z	377

TABLE III.—DIRECTION COSINE TABLE

New coordinate system	Old coordinate system		
	x	y	z
x'	$\lambda_{x'x}$	$\lambda_{x'y}$	$\lambda_{x'z}$
y'	$\lambda_{y'x}$	$\lambda_{y'y}$	$\lambda_{y'z}$
z'	$\lambda_{z'x}$	$\lambda_{z'y}$	$\lambda_{z'z}$

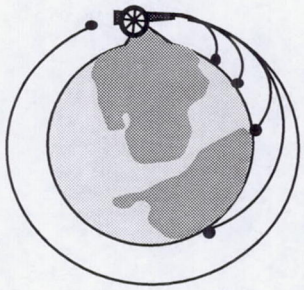

Figure 1.—Orbital cannonball concept.

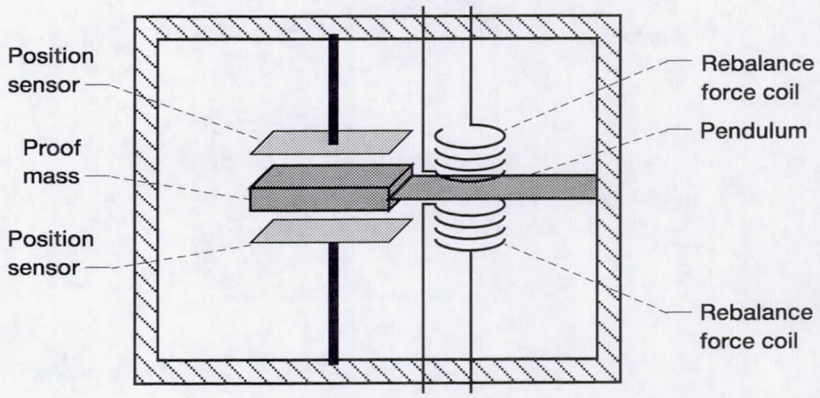

Figure 2.—Pendulous mass acceleration sensor (single axis).

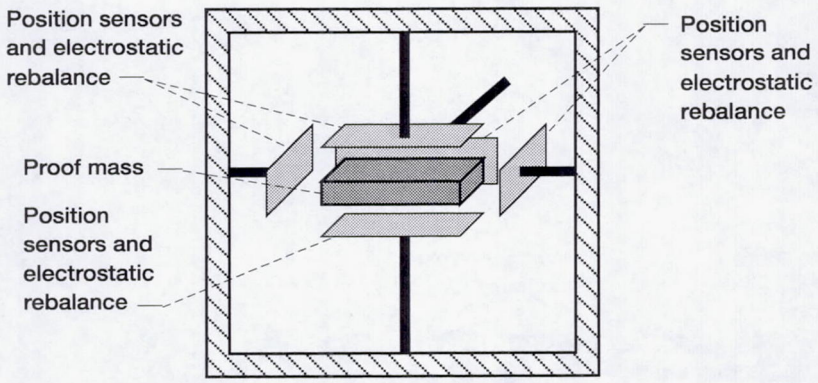

Figure 3.—Electrostatically suspended acceleration sensor (three axes.)

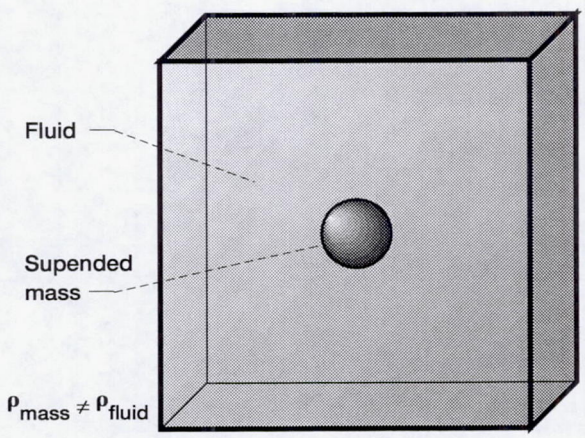

Figure 4.—Fluid suspended mass sensor.

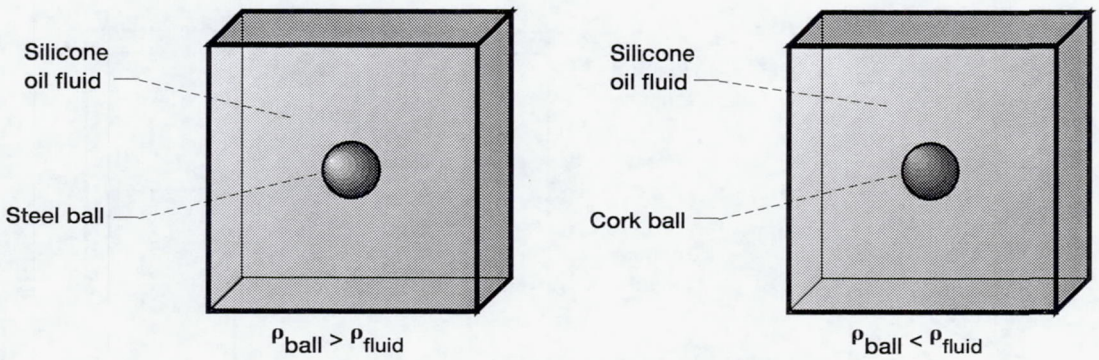

Figure 5.—Forward and reverse polarity fluidic sensor.

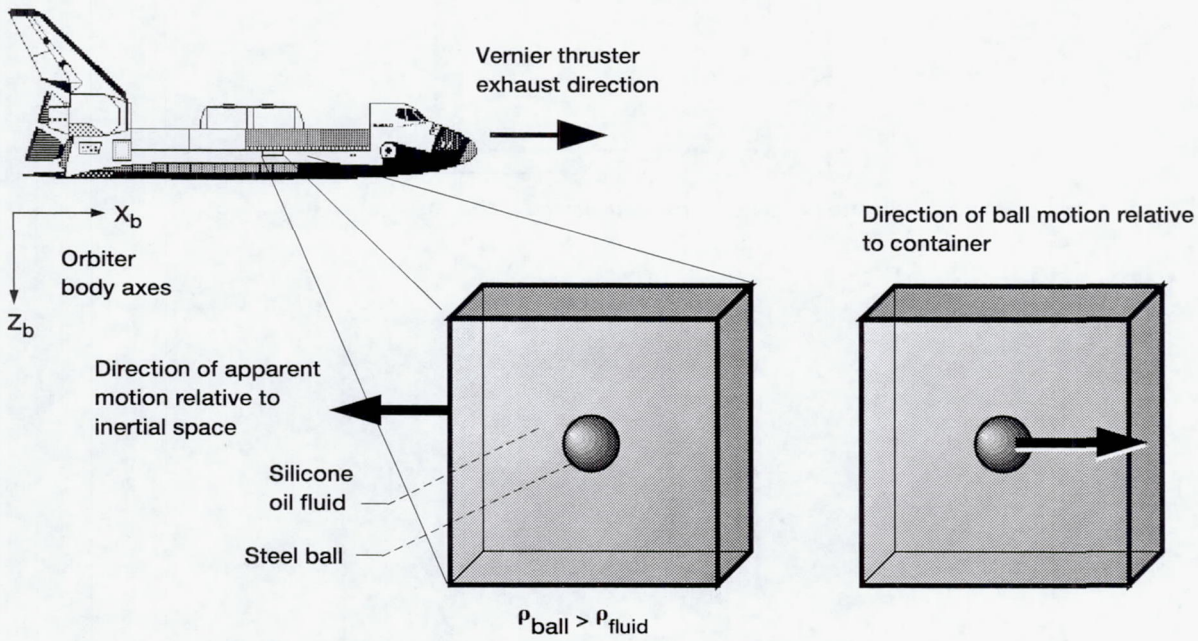

Figure 6.—Mobile tracer particle in fluid.

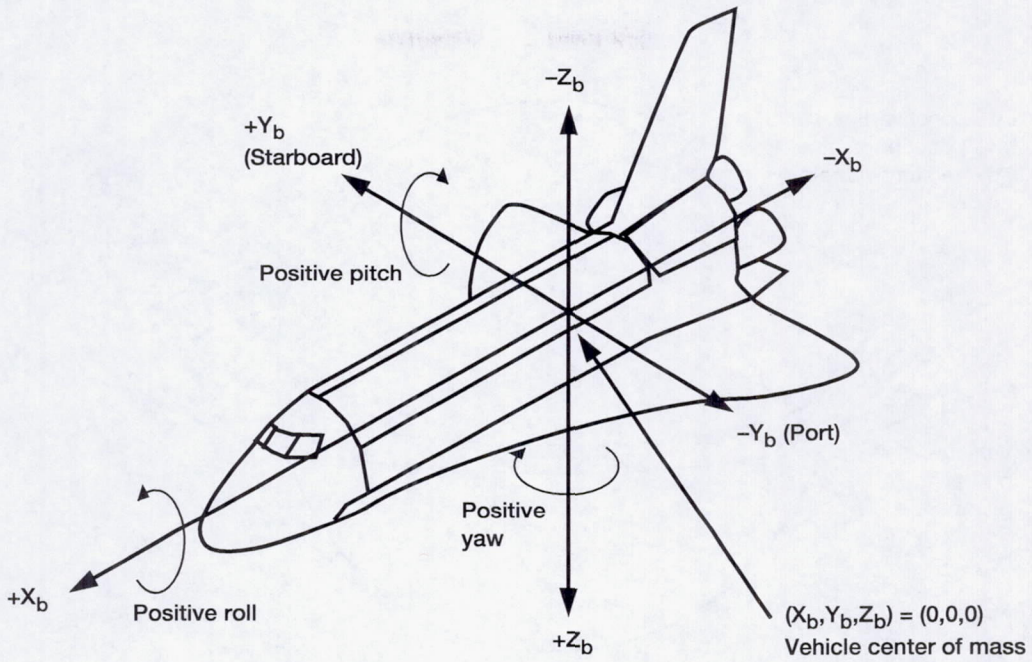

Figure 7.—Orbiter body coordinate system.

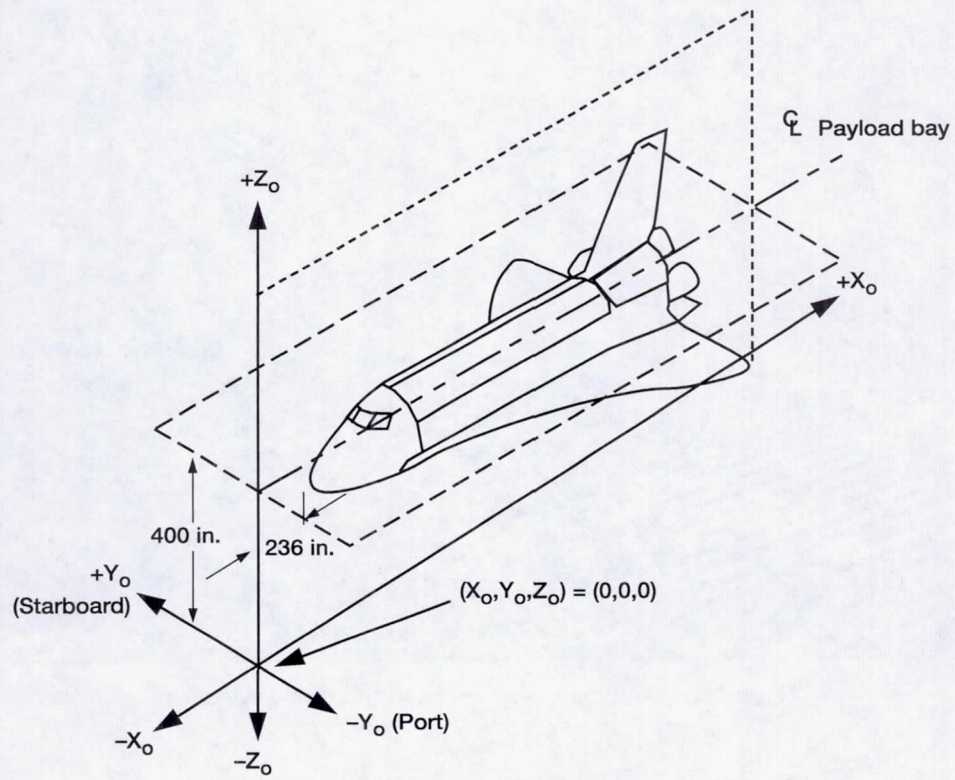

Figure 8.—Orbiter structural coordinate system.

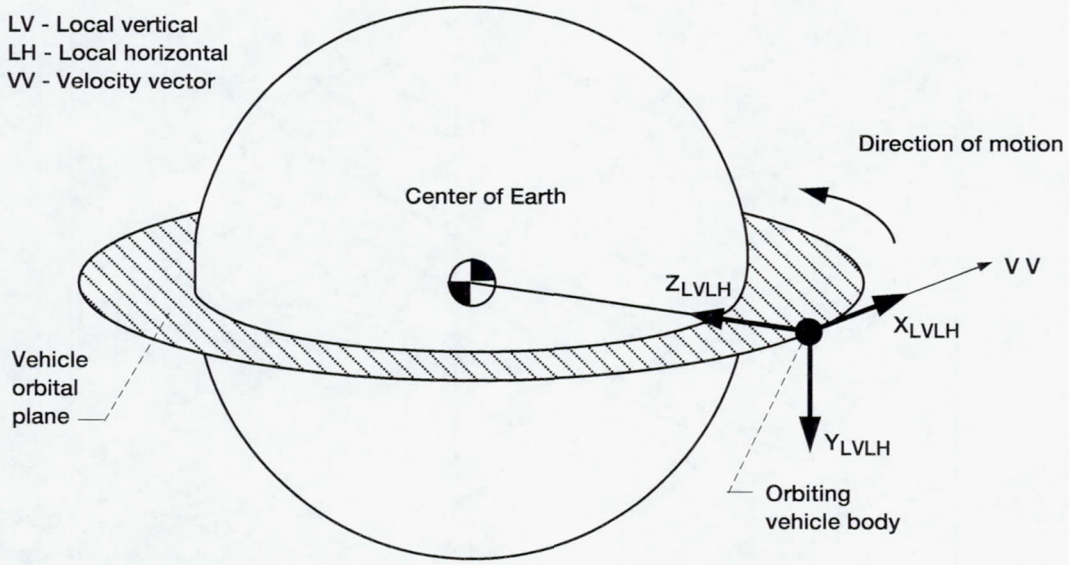

Figure 9.—Orbiter local vertical/local horizontal coordinate system.

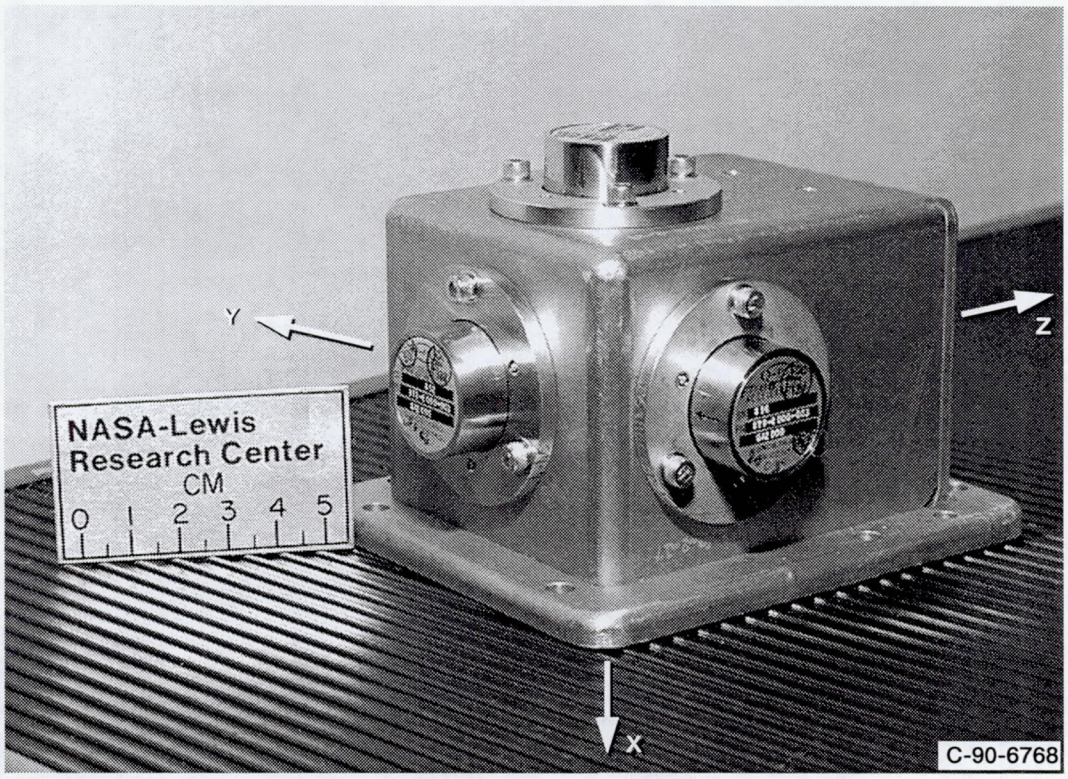

Figure 10.—SAMS triaxial sensor head coordinate system.

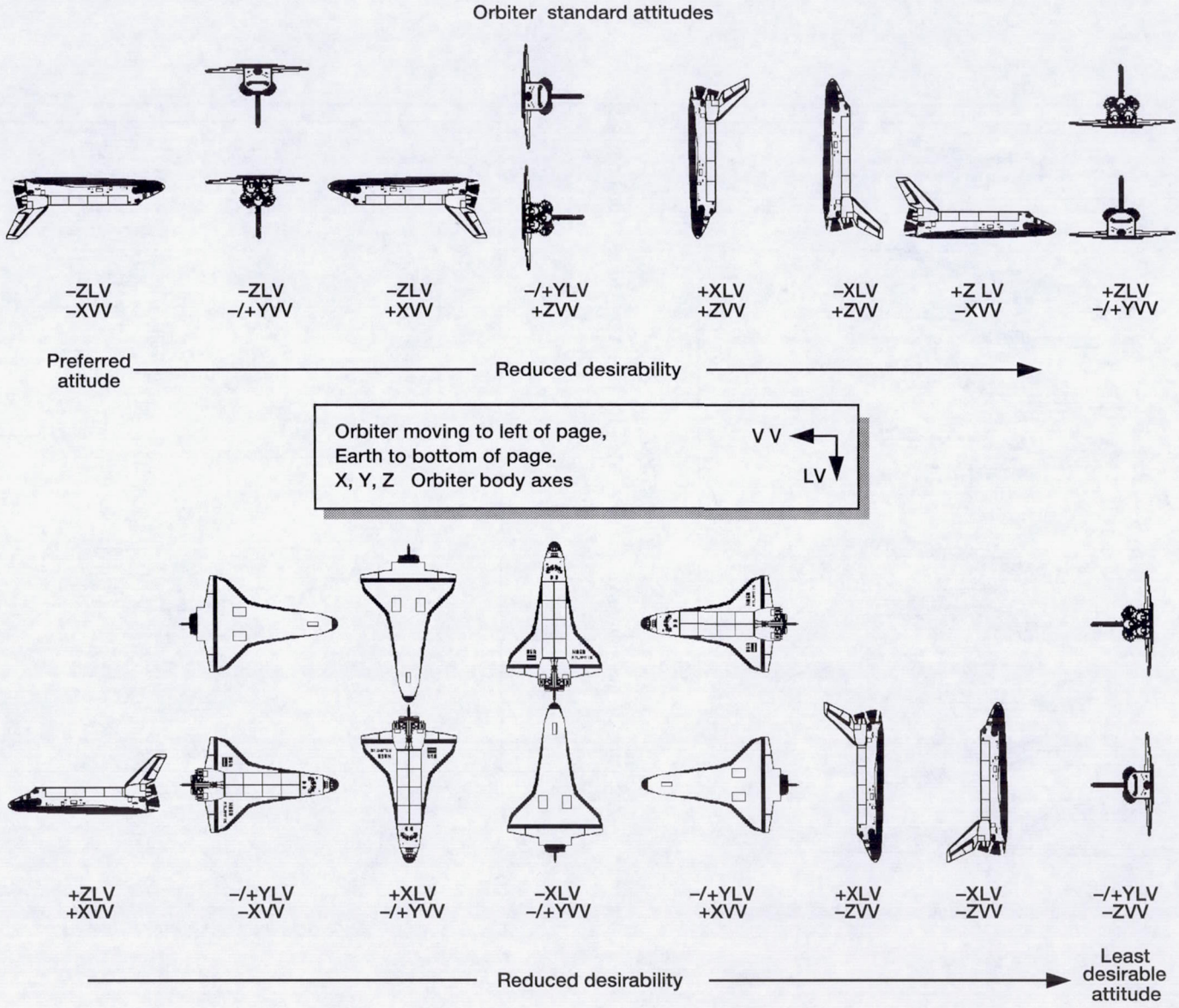

Figure 11.—Orbiter local vertical/local horizontal attitudes.

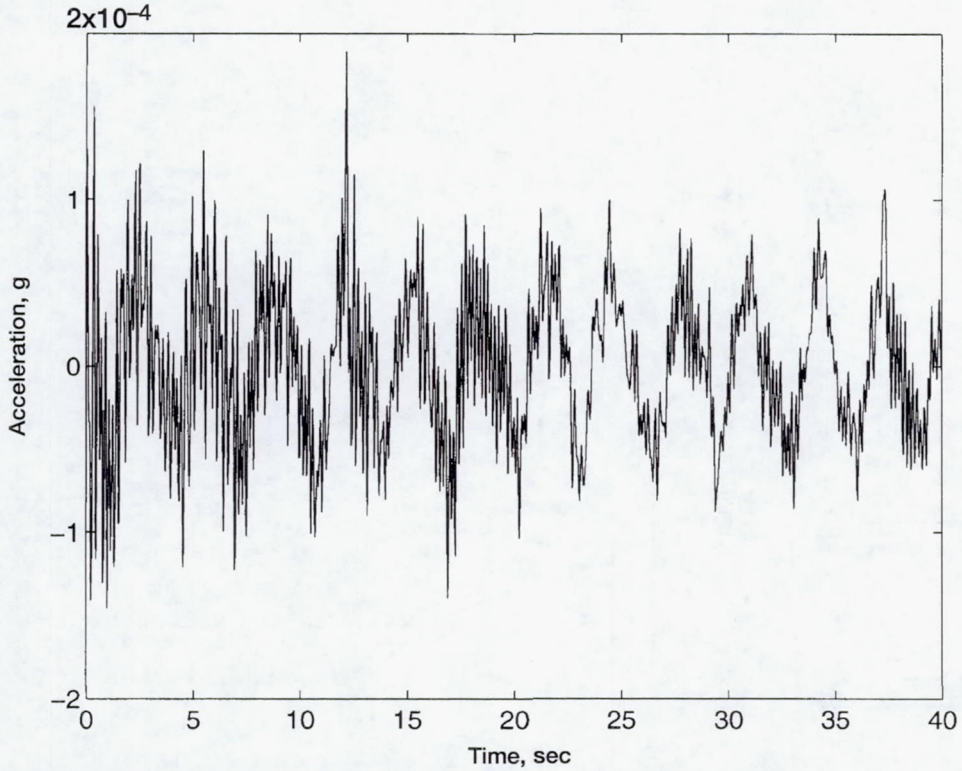

Figure 12.—Acceleration magnitude versus time. STS–40, TSH-A, X-axis, SET 003/03:18:50.

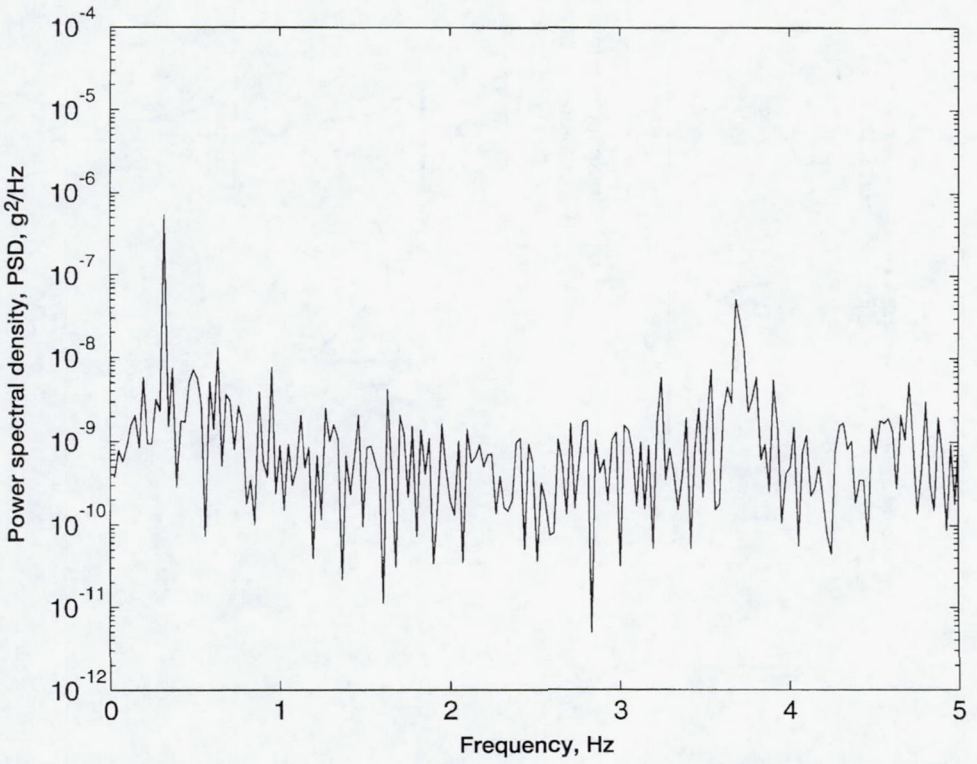

Figure 13.—Acceleration vector magnitude versus frequency. STS–40, TSH-A, X-axis, SET 003/03:18:50, 40 sec.

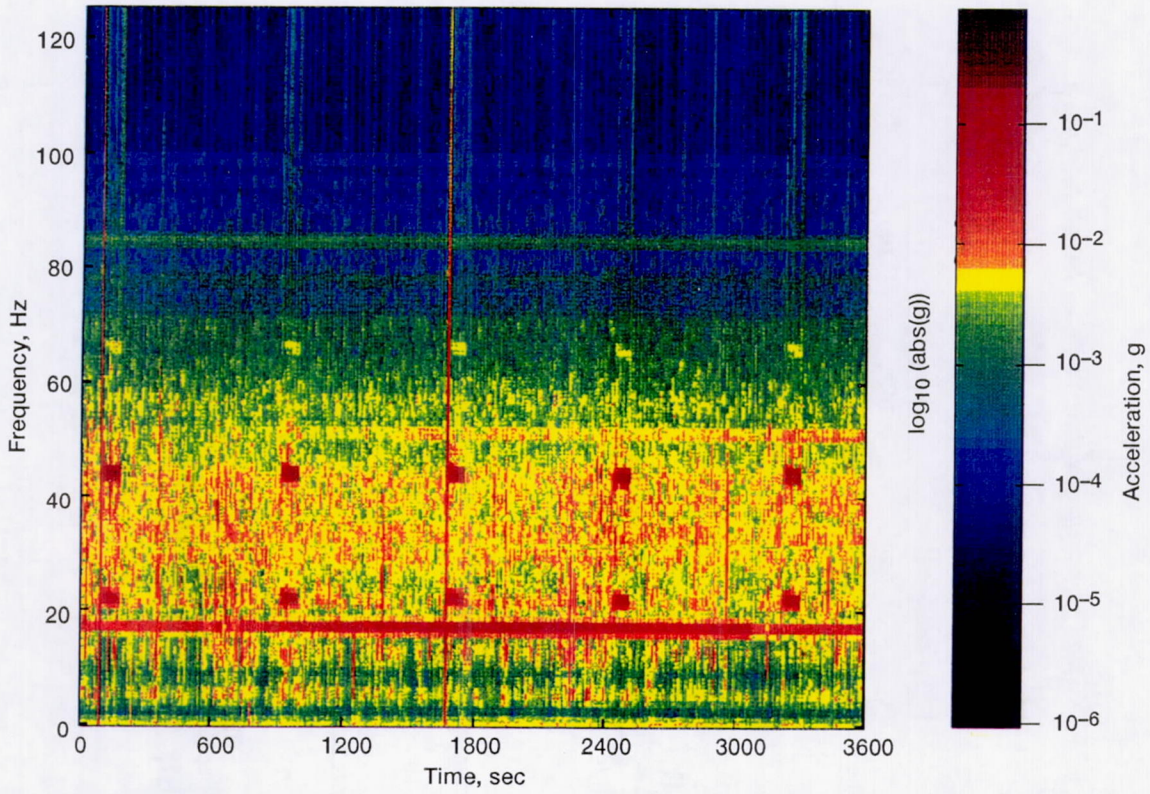

Figure 14.—Acceleration magnitude versus time verse frequency. STS–47, TSH-A, MET 000/23:00:00, 1 hr, fc = 50 Hz; 250 s/s.

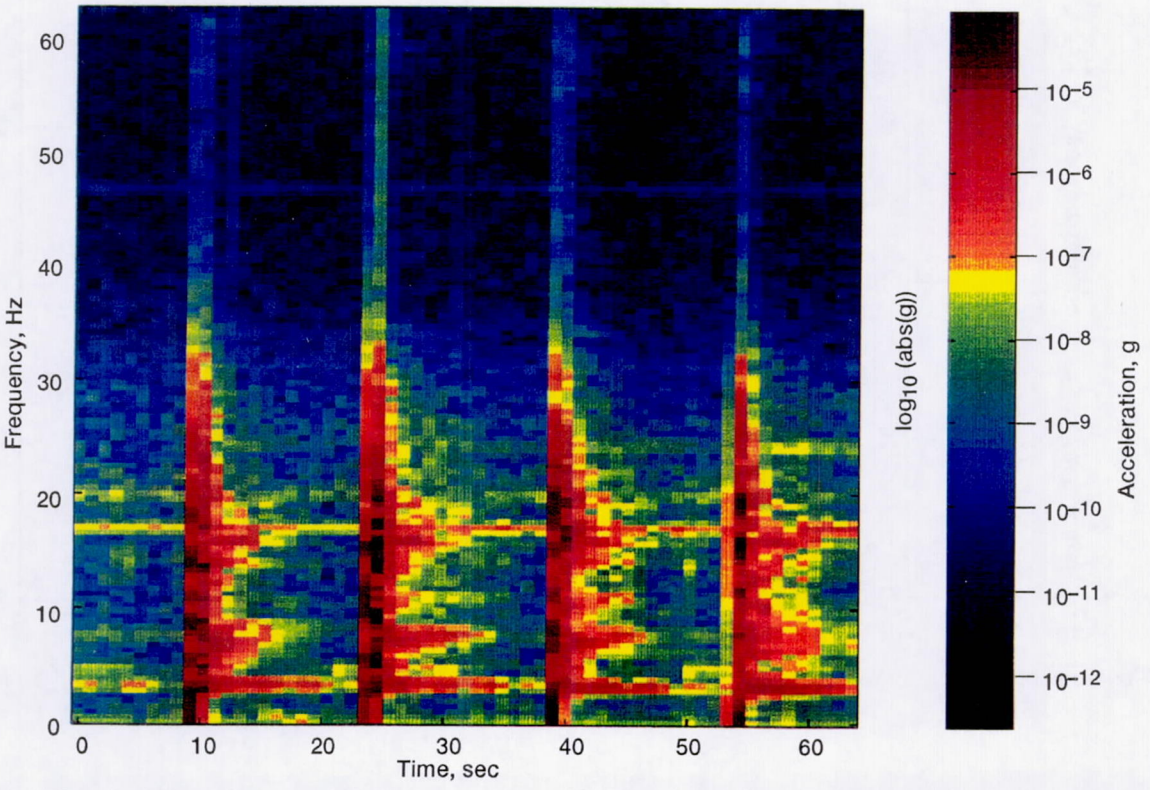

Figure 18.—Thruster disturbance over wide-frequency band. STS–62, TSH-B, MET 010/17:14:20, 66 sec, fc = 25 Hz; 250 s/s.

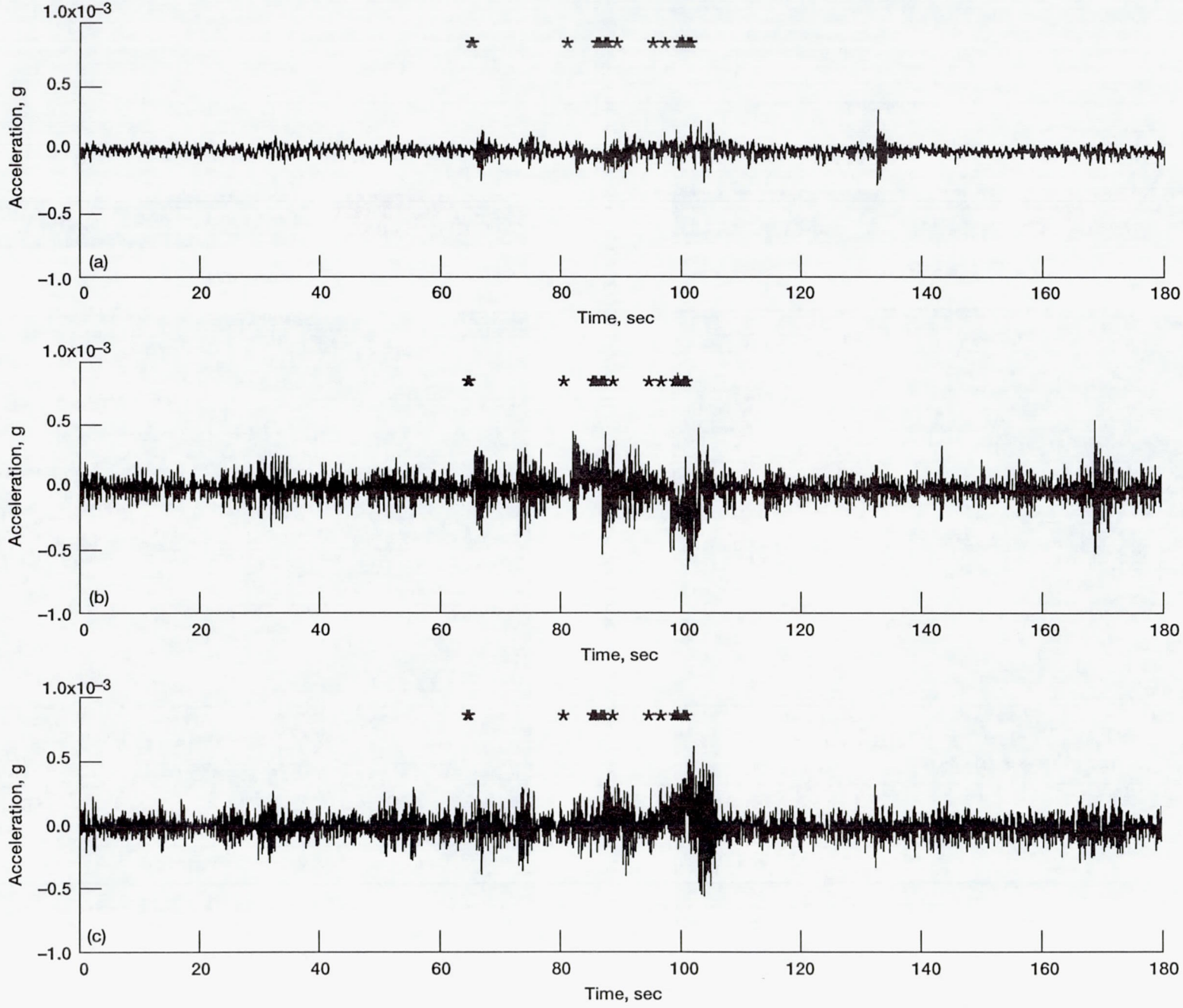

Figure 15.—Vernier Reaction Control System thruster acceleration signature. STS–65, TSH-A, MET 006/10:08:40. (a) X-axis. (b) Y-axis. (c) Z-axis.

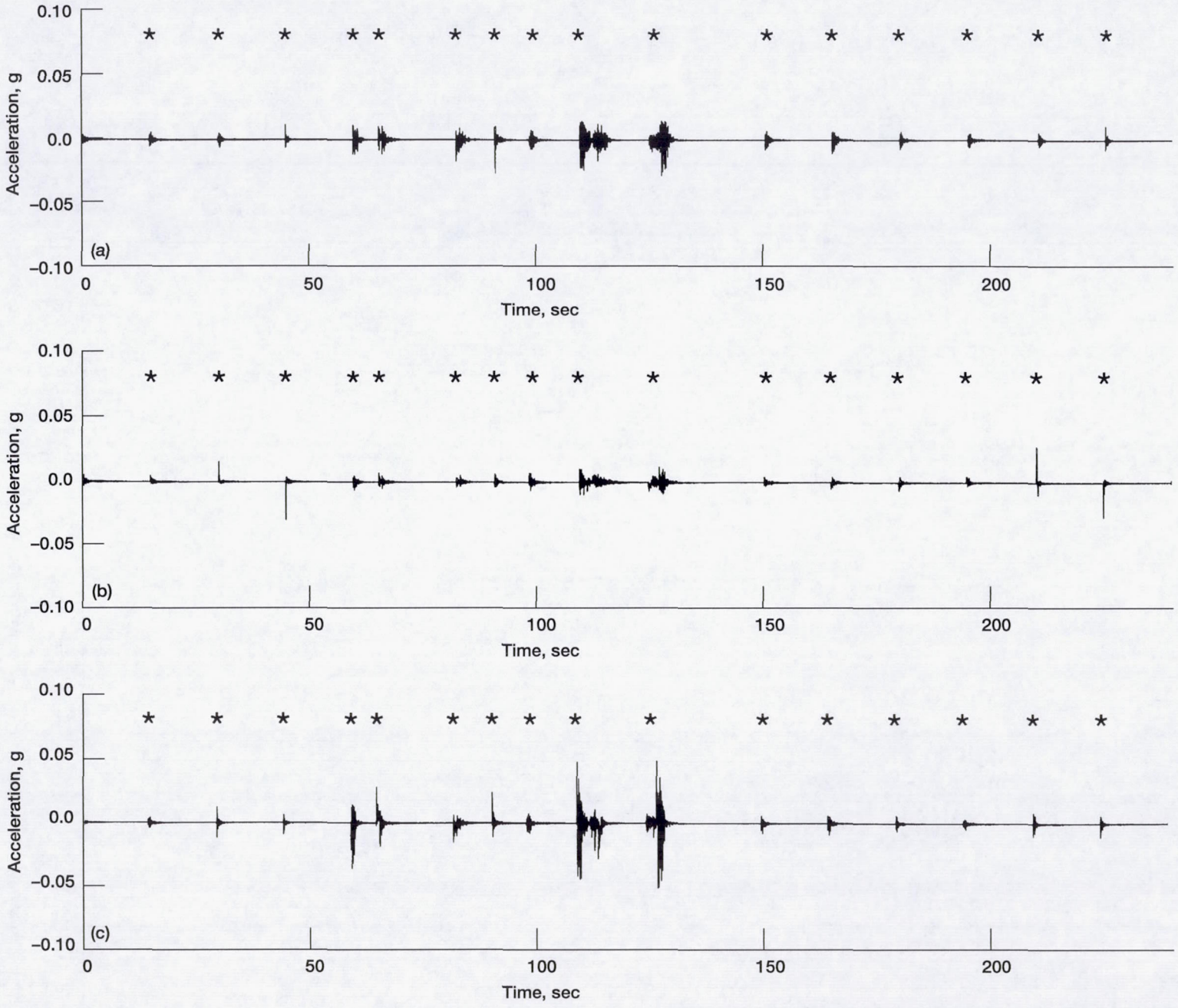

Figure 16.—Primary Reaction Control System thruster acceleration signature. STS–62, TSH-B, MET 010/17:12:00. (a) X-axis. (b) Y-axis. (c) Z-axis.

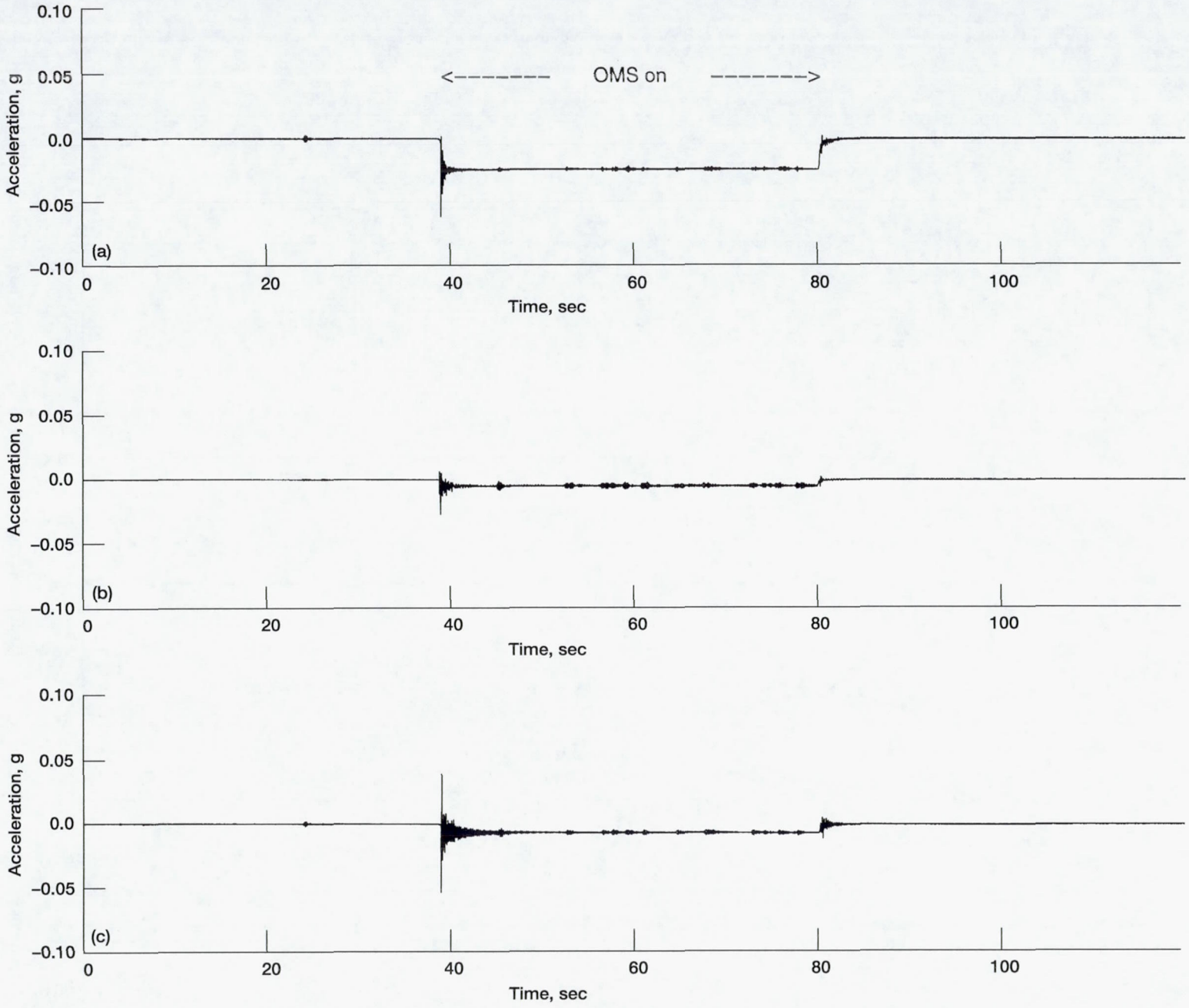

Figure 17.—Orbital Maneuvering System (OMS) thruster acceleration signature. STS–62, TSH-B, MET 009/17:09:00. (a) X-axis. (b) Y-axis. (c) Z-axis.

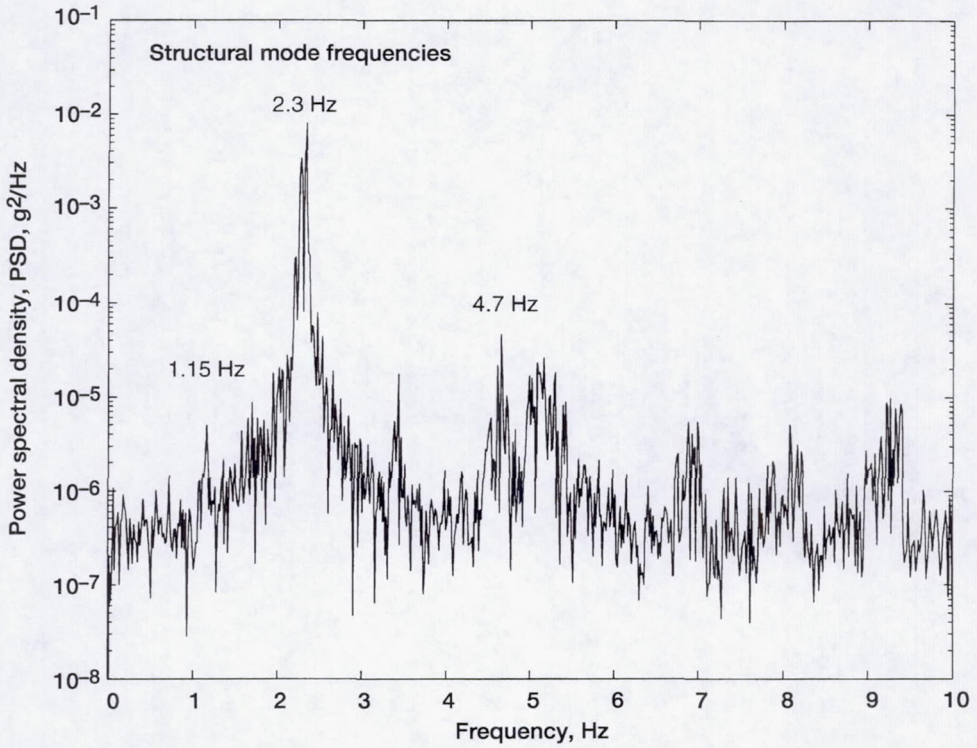

Figure 19.—Crew exercise on treadmill. STS–43, TSH-A, MET 001/07:17:10, 66 sec.

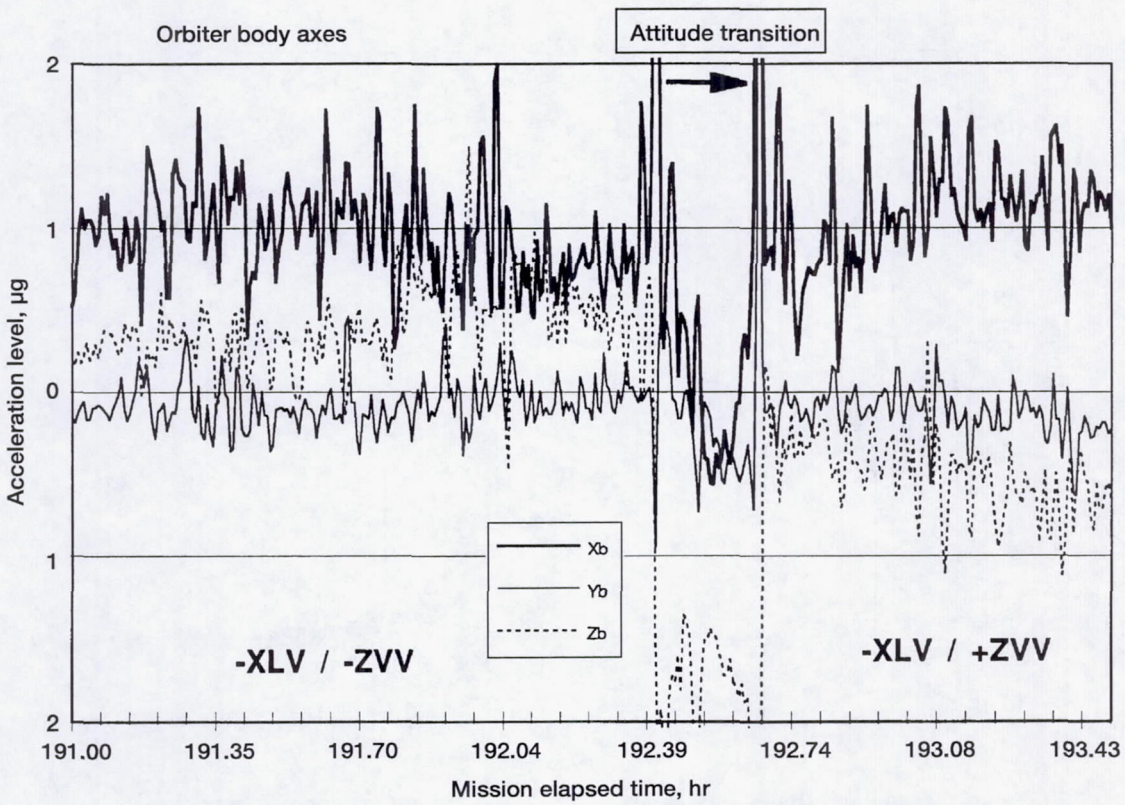

Figure 20.—Quasi-steady acceleration before, during, and after Orbiter maneuver.

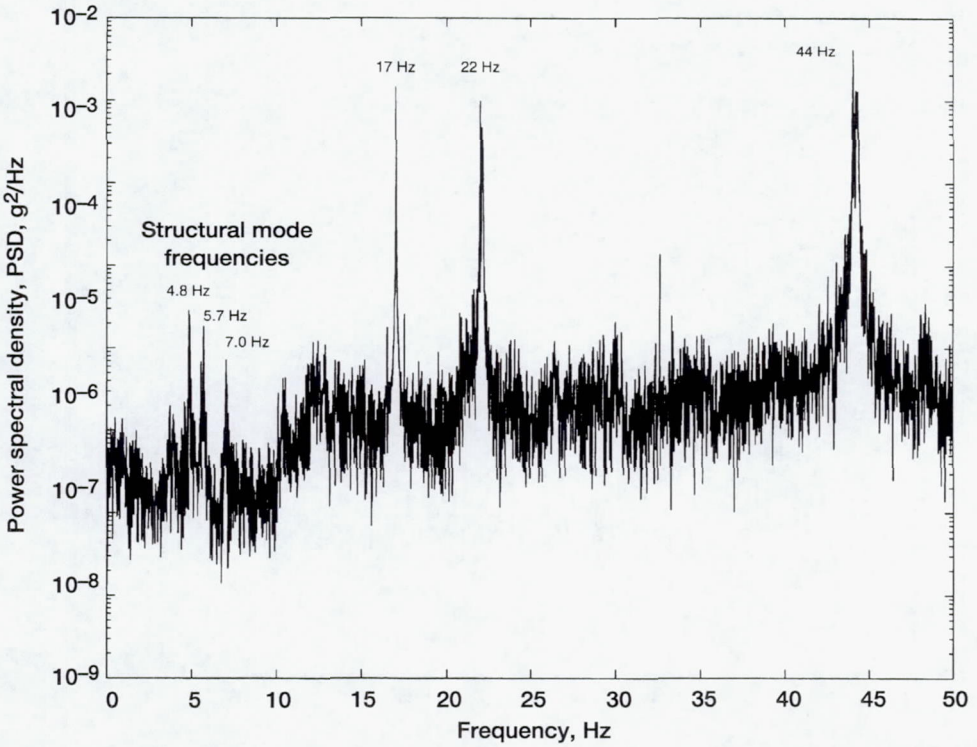

Figure 21.—Antenna and refrigerator/freezer operating frequencies. STS–47, TSH-A, MET 000/23:28:04, 66 sec.

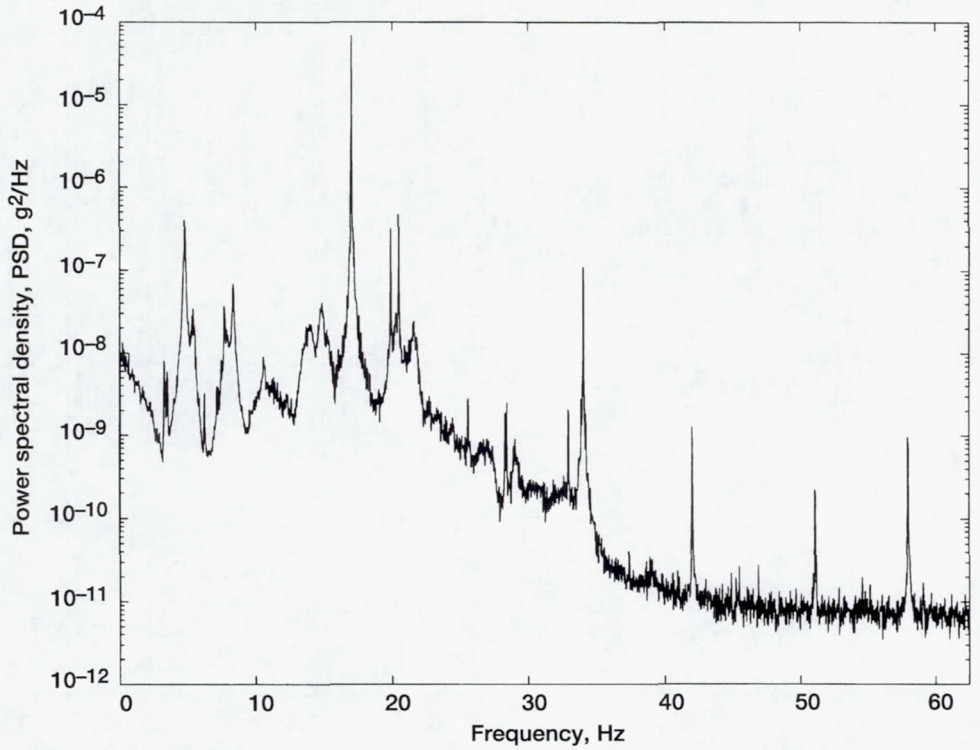

Figure 22.—Antenna dither frequency with first and second harmonic frequencies. STS–62, TSH-B, MET 008/09:53:16, 8 min 44 sec, fc = 25 Hz, 125 s/s.

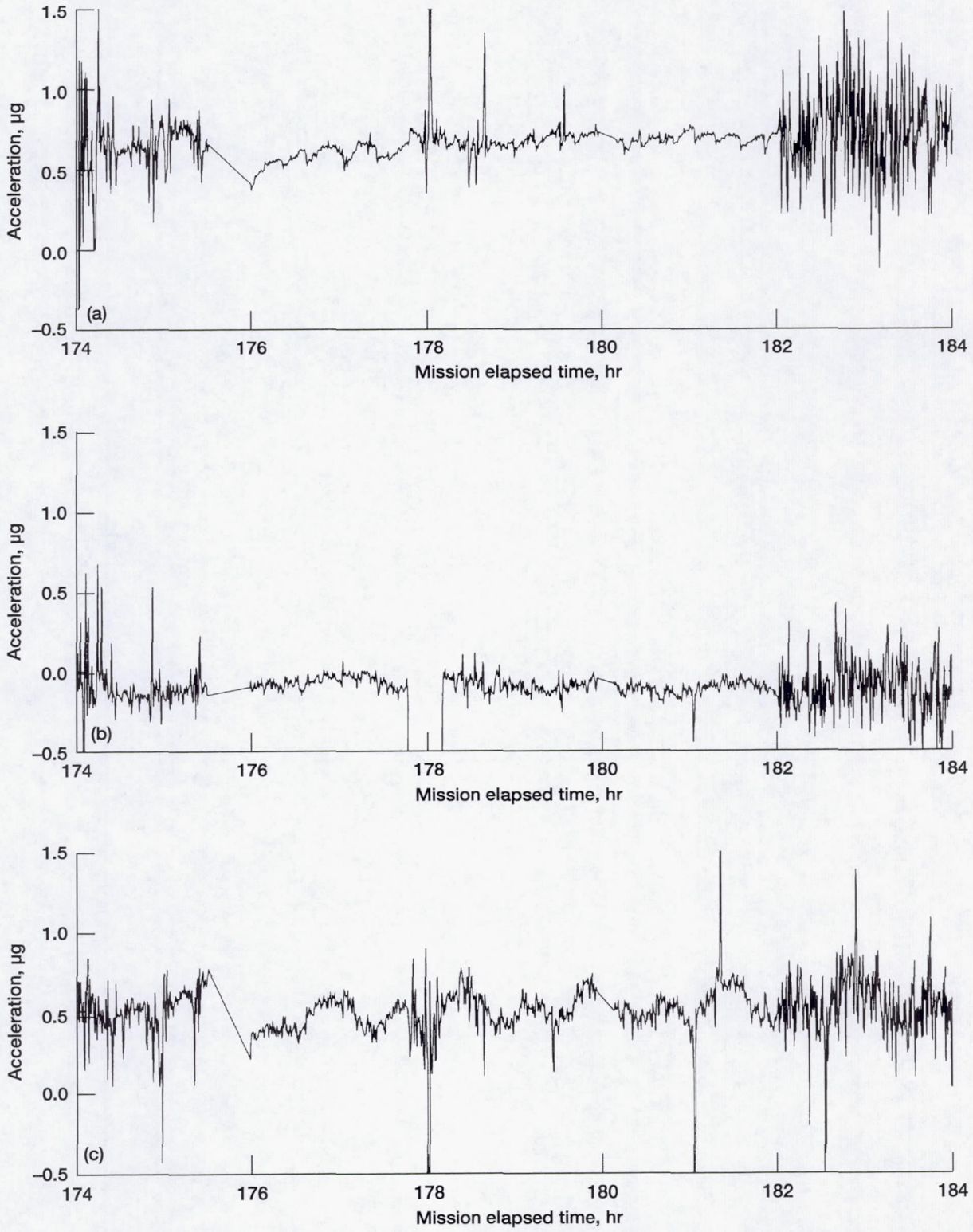

Figure 23.—Acceleration magnitude variation at orbital period with near-circular orbit. (a) X-axis. (b) Y-axis. (c) Z-axis.

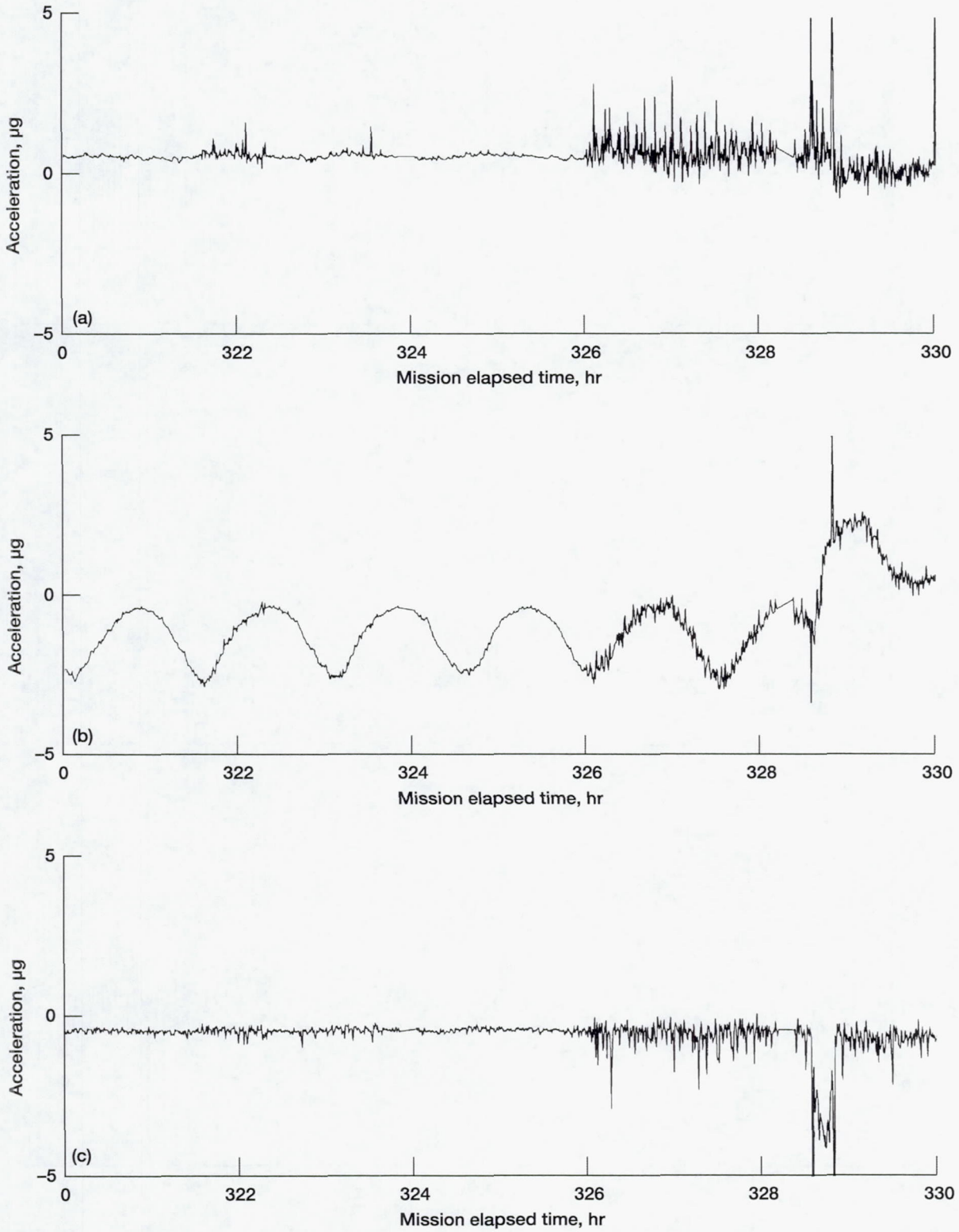

Figure 24.—Acceleration magnitude variation at orbital period with elliptical orbit. (a) X-axis. (b) Y-axis. (c) Z-axis.

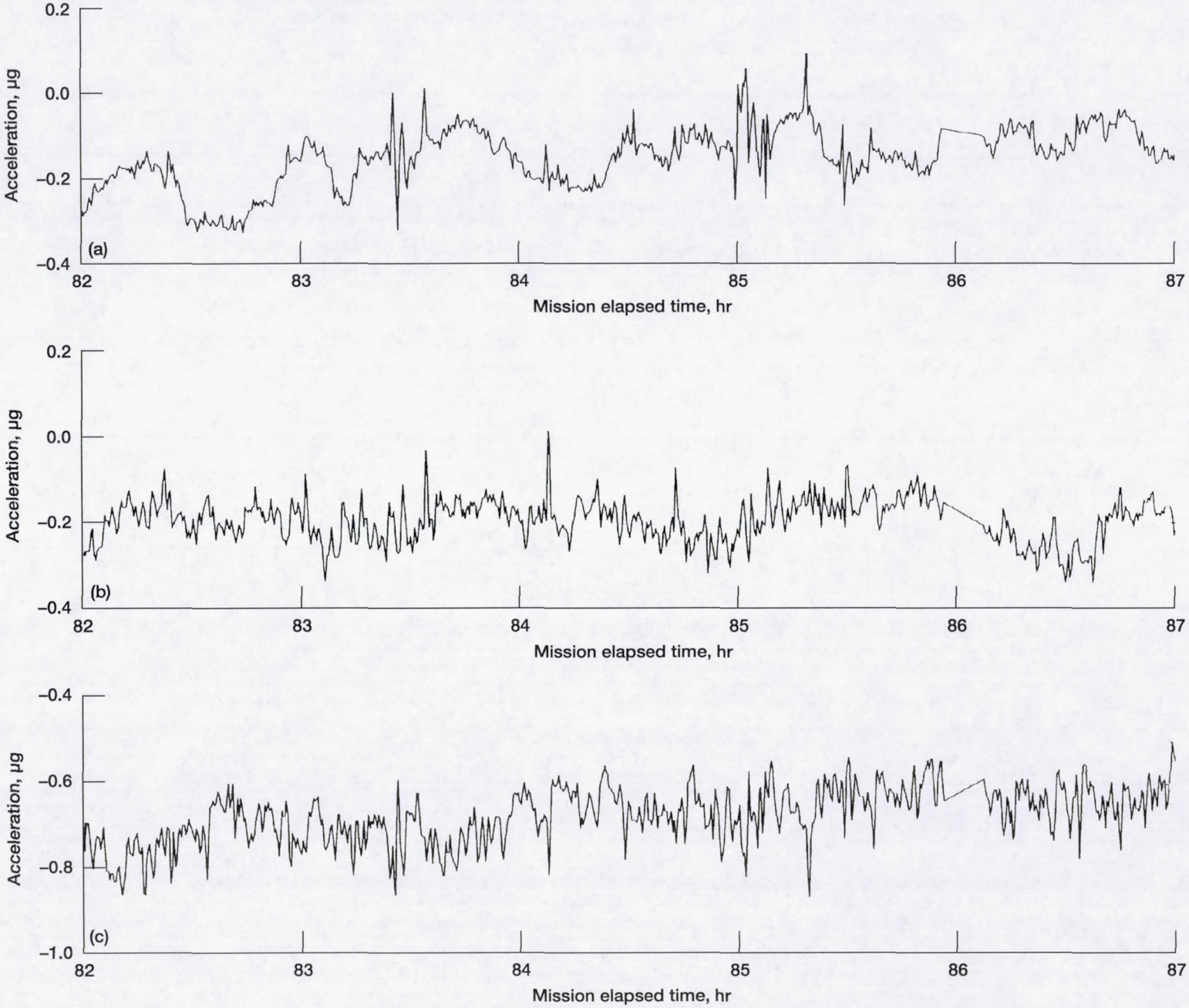

Figure 25.—Acceleration magnitude at OARE location. (a) X-axis. (b) Y-axis. (c) Z-axis.

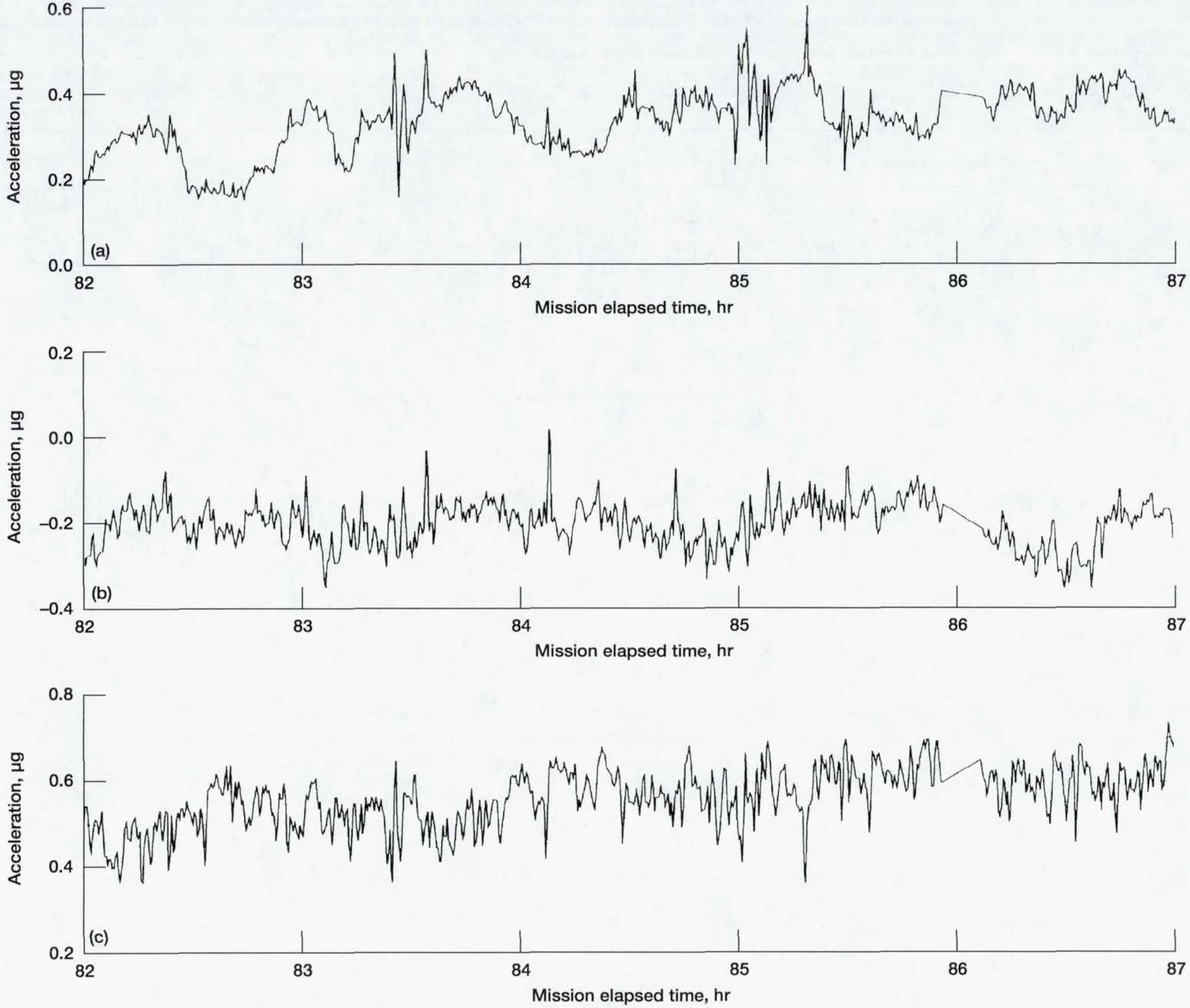

Figure 26.—Acceleration magnitude at IDGE location. (a) X-axis. (b) Y-axis. (c) Z-axis.

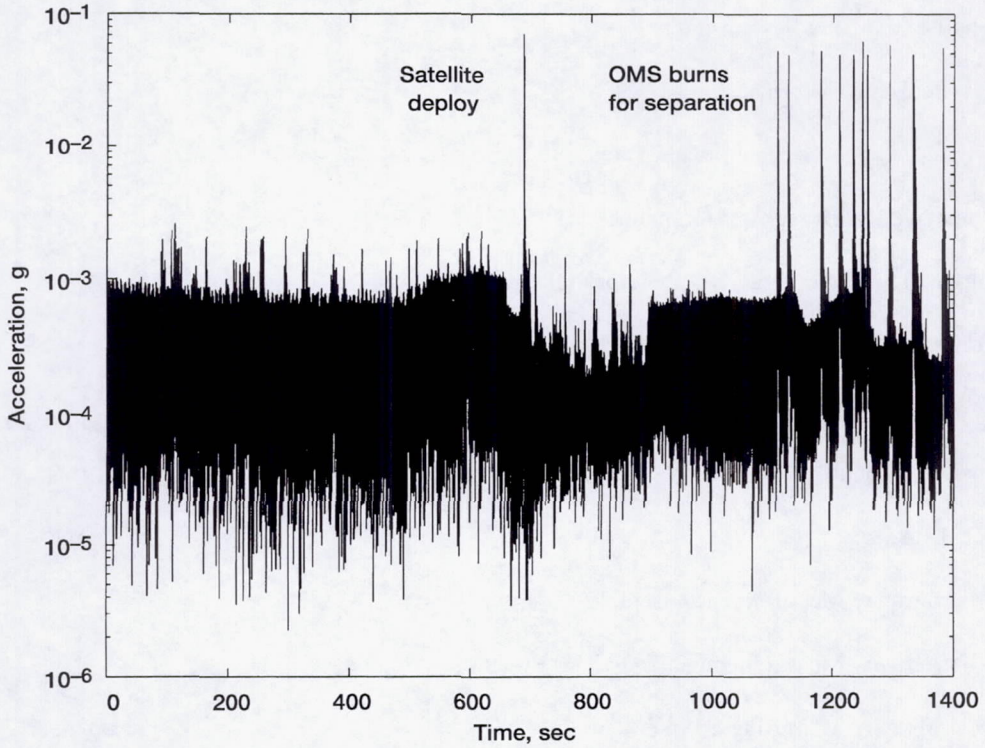

Figure 27.—LAGEOS satellite launch. STS–52, TSH-B, vector magnitude, MET 000/20:36:00.

APPENDIX A—ACRONYMS

3DMA	Three-Dimensional Microgravity Accelerometer
CD-ROM	compact disk read only memory
CG	center of gravity
CM	center of mass
DLR	Deutsche Forschungsanstalt fur Luft und Raumfahrt
FES	Fluid Experiment System
FFT	fast Fourier transform
HiRAP	High Resolution Accelerometer Package
HISA	Honeywell In-Space Accelerometer
IML	International Microgravity Laboratory mission series
JSC	Johnson Space Center
LeRC	Lewis Research Center
LH	local horizontal
LV	local vertical
MMA	Microgravity Measurement Assembly
MMAP	Microgravity Measurement and Analysis Project
MMD	Microgravity Measuring Device
MPESS	Mission Peculiar Equipment Support Structure
MSAD	Microgravity Science and Applications Division
MSFC	Marshall Space Flight Center
NRT	near-real-time
OARE	Orbital Acceleration Research Experiment
OMS	Orbital Maneuvering System
PAS	Passive Accelerometer System
PI	Principal Investigator
PIMS	Principal Investigator Microgravity Services

POCC	Payload Operations Control Center
PRCS	Primary Reaction Control System
PSD	power spectral density
QSAM	Quasi-Steady Acceleration Measurement
RCS	Reaction Control System
RMS	Remote Manipulator System
rms	root mean square
SAMS	Space Acceleration Measurement System
SL-D-2	Second German Spacelab mission
SL-J	Spacelab J mission
SLS	Spacelab Life Sciences mission series
STS	Space Transportation System
TSH	triaxial sensor head
UAH	University of Alabama in Huntsville
USML	United States Microgravity Laboratory mission series
USMP	United States Microgravity Payload mission series
VRCS	Vernier Reaction Control System
VV	velocity vector
WSF	Wake Shield Facility

APPENDIX B—DEFINITIONS

The meaning of the following terms is necessary for an understanding of this document:

g_o	an acceleration equal to the normal Earth's gravitational acceleration at sea level (nominally 9.8 m/sec^2).
mg or milli-g	an acceleration equal to one thousandth of the normal Earth's gravitational acceleration at sea level ($g_o \times 10^{-3}$)
μg or micro-g	an acceleration equal to one millionth of the normal Earth's gravitational acceleration at sea level ($g_o \times 10^{-6}$)
I_{sp}	specific impulse
X_b, Y_b, Z_b	components of the Orbiter body coordinate system
X_{LVLH}, Y_{LVLH}, Z_{LVLH}	components of the local vertical/local horizontal coordinate system
X_o, Y_o, Z_o	components of the Orbiter structural coordinate system
ρ_{ball}	density of a ball
ρ_{fluid}	fluid density
ρ_{mass}	density of a mass

APPENDIX C—ACCESSING SAMS DATA FILES VIA INTERNET

SAMS data are distributed on CD-ROM media and are available on a computer file server. In both cases, files of SAMS data are organized in a treelike structure as illustrated in figure C1. Data acquired from a mission are categorized by sensor head, mission day, and type of data. Data files are stored at the highest level in the tree, and the file name reflects the contents of the file. For example, the file named `axm00102.15r` contains data for sensor head A, the X-axis, the time base was Mission Elapsed Time, day 001, hour 02, 1 of 5 files for that hour, and it contains reduced data. The file readme.doc provides a comprehensive description and guide to the data.

Also available from the file server are some data access tools for different computer platforms.

SAMS data files may be accessed from a file server at NASA LeRC. The NASA LeRC file server `beech.lerc.nasa.gov` can be accessed via anonymous file transfer protocol (ftp), as follows:

(1) Establish ftp connection to the beech file server.
(2) Login: `anonymous`
(3) Password: `guest`
(4) Change the directory to: `pub`
(5) List the files and directories in the pub directory.
(6) Change the directory to the mission of interest, for example: `usml-1`
(7) List files and directories for the specific mission chosen in previous step.
(8) Use the data file structure shown in the figure to find the files of interest.
(9) Transfer the data files of interest.

If you encounter difficulty in accessing the data using the file server, please send an electronic mail message to the following Internet address: `pims@lerc.nasa.gov`. Please describe the nature of the difficulty and a description of the hardware and software you are using to access the file server.

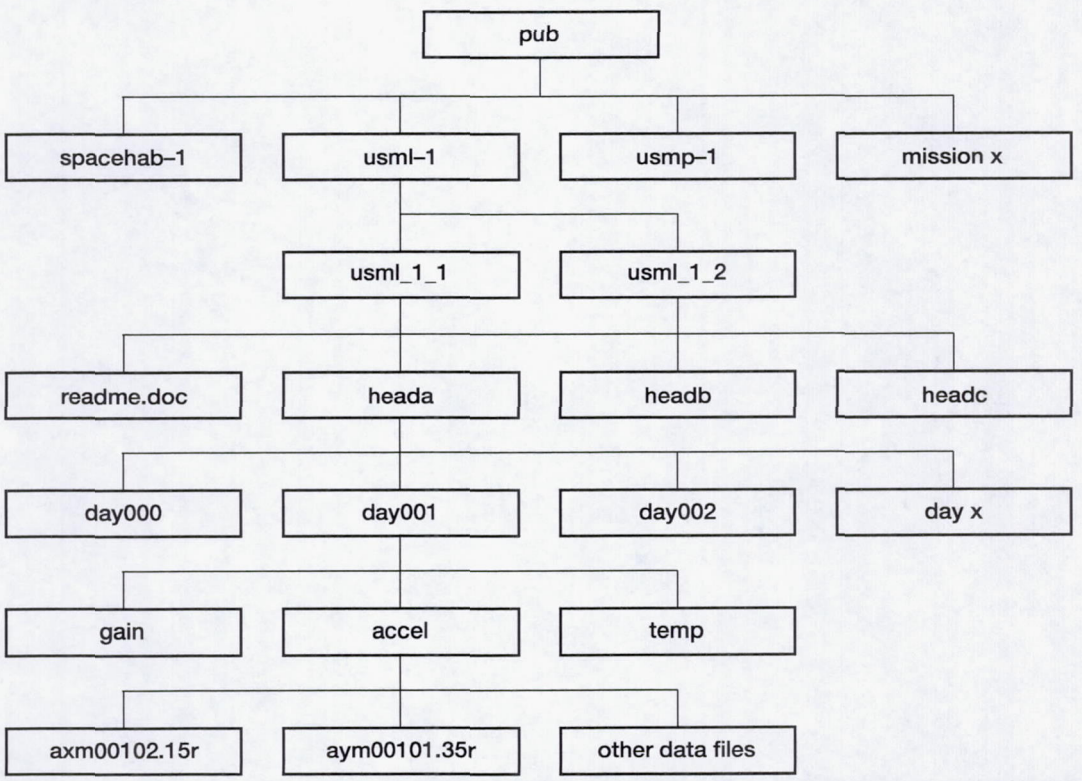

Figure C1.—SAMS data file structure.

APPENDIX D—RCS AND OMS ENGINES DESCRIPTION [1]

Reaction Control System (RCS)

The reaction control system (RCS) consists of 44 individual thrusters located in three separate modules in the Orbiter (forward, aft-left, and aft-right). There are 38 primary jets and 6 vernier jets. Each primary jet is rated at 870 lb of thrust, and each vernier jet is rated at 24 lb of thrust. The primary jets are used to control the motion of the space shuttle vehicle through a combination of translation and/or rotational movement. The vernier jets are used on orbit for fine attitude control. The locations of the RCS thrusters in relationship to the Orbiter are shown in figure D1, and details of the jet locations and plume directions are shown in figure D2. While most thrusters are aligned with the Orbiter body axes, it should be noted that many of the thrusters in the forward module are off-axis. This is further illustrated in figure D3. The 6 vernier thrusters are shown in figure D2 as F5R, F5L, L5L, L5D, R5R, and R5D.

Orbital Maneuvering System (OMS)

The OMS engines provide propulsion for the space shuttle vehicle during the orbit phase of flight. They are used for orbital insertion maneuvers after the main propulsion system has shut down. They are also the primary propulsion system for orbital transfer maneuvers and the de-orbit maneuver.

There are two OMS engines per Orbiter. Each OMS engine produces 6000 lb of thrust. The locations of the OMS engines in relationship to the Orbiter are shown in figure D1. The OMS engines are canted 15.8° upward and 6.5° outboard with respect to the Orbiter body axes. The OMS engines can be pivoted up and down (±6°) and from side to side (±7°) from their null position.

[1]Reprinted from Appendix B of NASA TP–3141 (ref. 4).

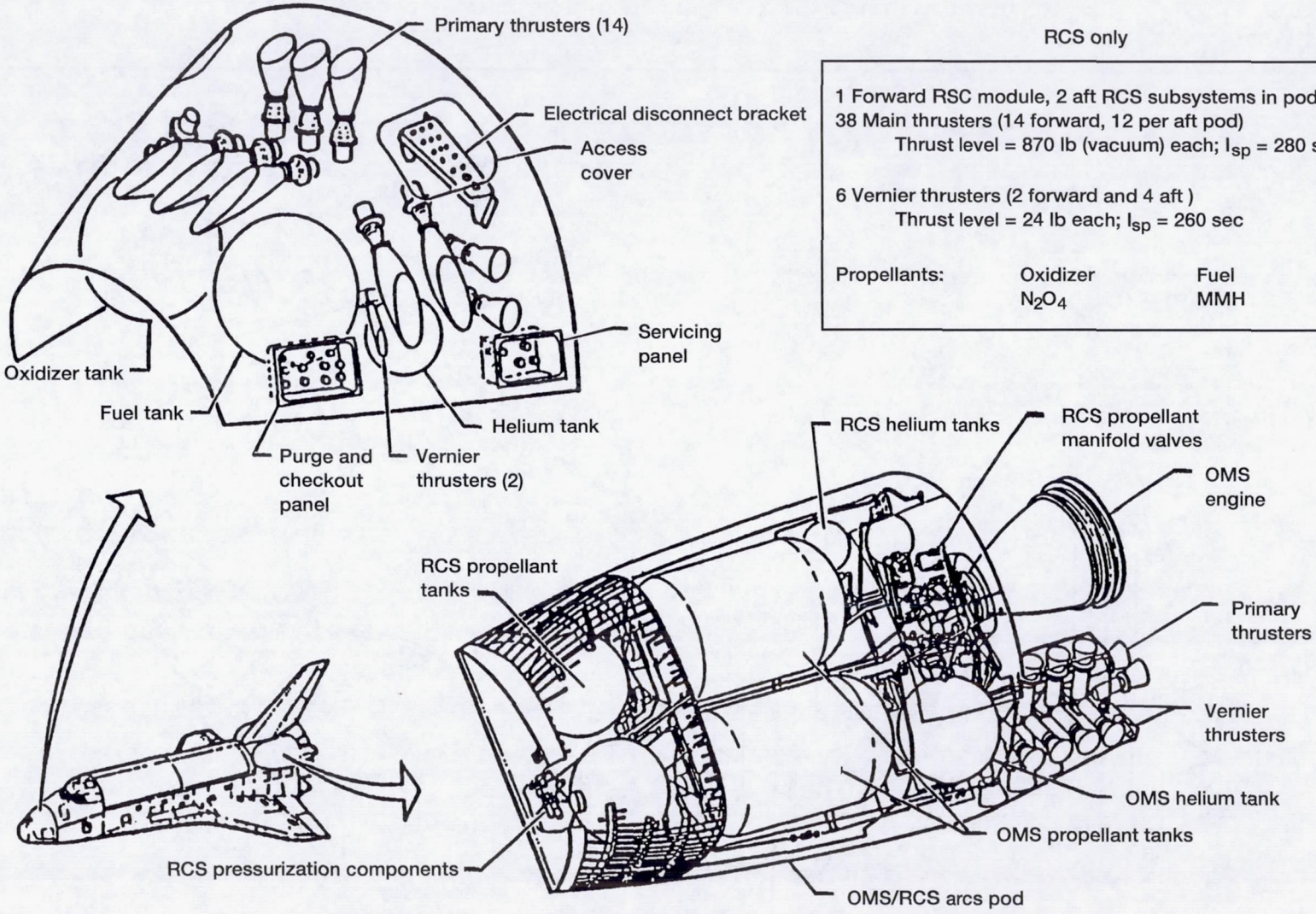

Figure D1.—Reaction Control System (RCS) thruster locations.

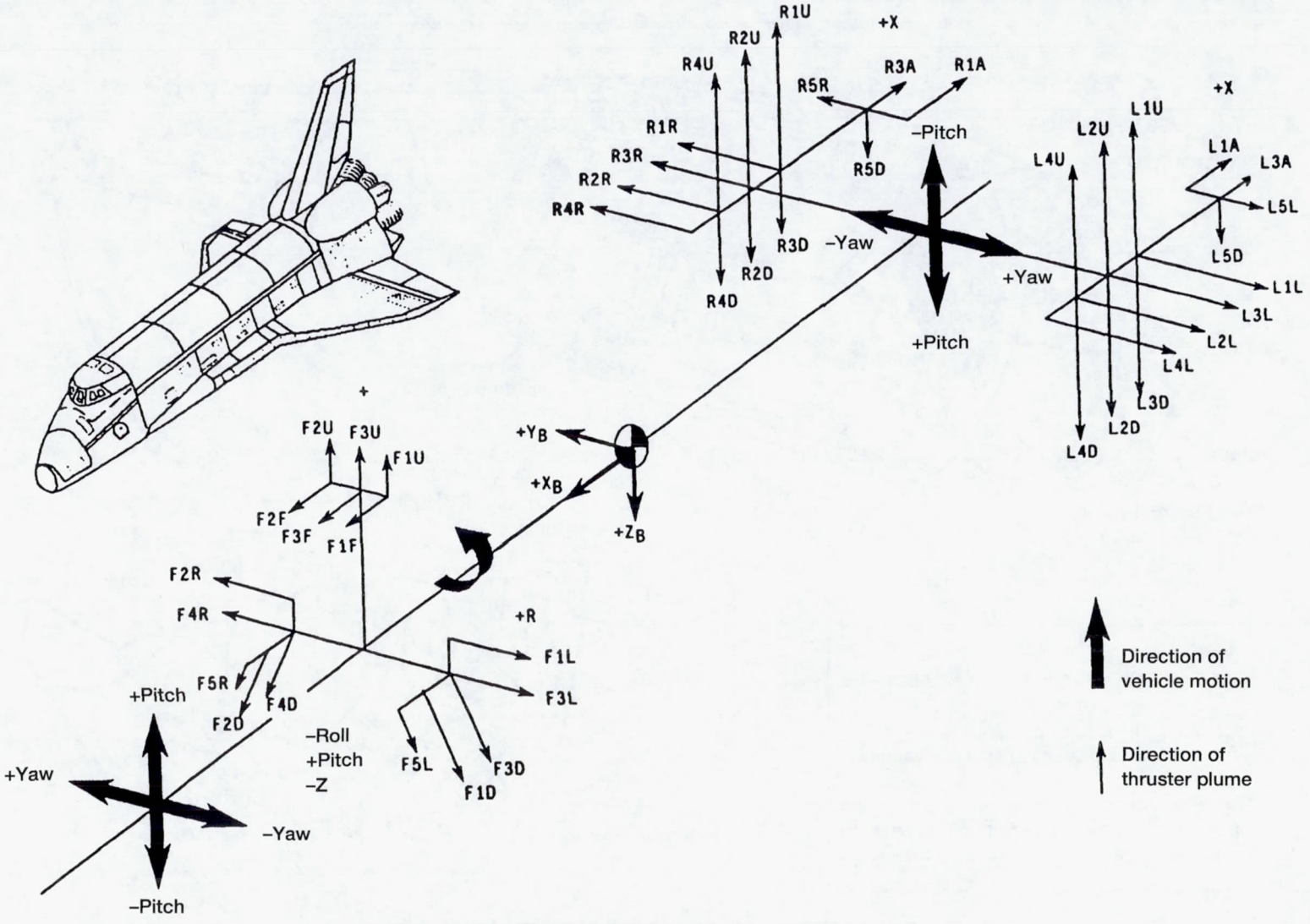

Figure D2.—Reaction Control System (RCS) jet locations and plume axes.

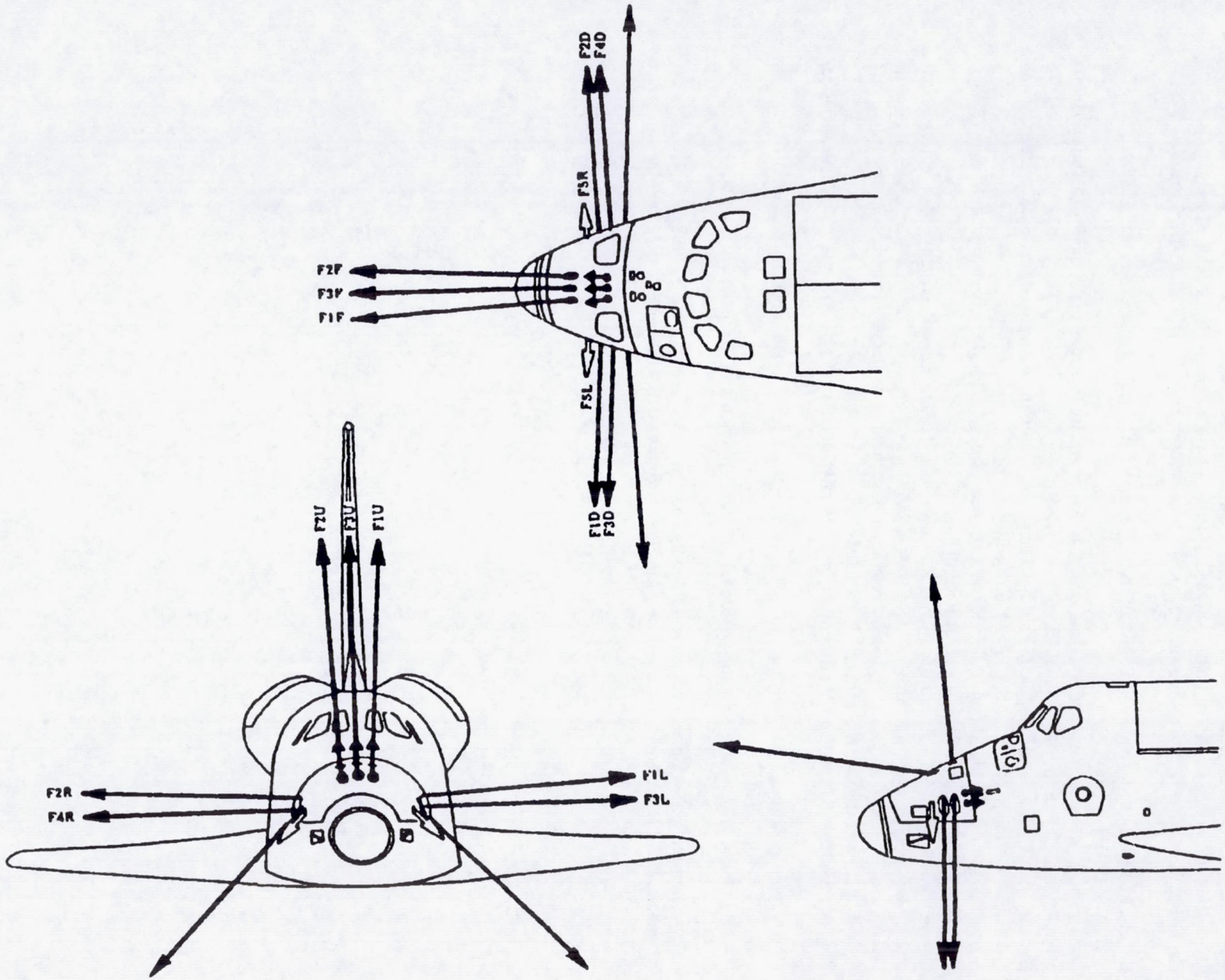

Figure D3.—Reaction Control System (RCS) jet locations and plume axes (detail drawing).

REFERENCES

1. Vogt, G.L.; Wargo, M.J.: Microgravity: A Teacher's Guide with Activities, Secondary Level. NASA EP-280, July 1992. (Available WWW Microgravity Home Page at http://microgravity.msad.hq.nasa.gov).
2. Hamacher, H.: Spacecraft Low-Frequency Residual Acceleration. Spac. Rock. vol. 32, no. 2, pp. 324–327, 1995.
3. Rogers, M.J.B.; and Alexander, J.I.D.: Analysis of Spacelab 3 Residual Acceleration Data. J. Spac. Rock., vol. 28, 1991, pp. 707–712.
4. Dunbar, B.J.; Giesecke, R.L.; and Thomas, D.A.: The Microgravity Environment of the Space Shuttle Columbia Payload Bay During STS–32. NASA TP–3141,1991.
5. Dunbar, B.J.; Thomas, D.A.; and Schoess, J.N.: The Microgravity Environment of the Space Shuttle Columbia Middeck During STS–32. NASA TP–3410, 1991.
6. Matisak, B.P.; Rogers, M.J.B.; and Alexander, J.I.D.: Analysis of the Passive Accelerometer System (PAS) Measurements During USML–1. AIAA Paper 94–0434, 1994.
7. DeLombard, R.; Finley, B.D.; and Baugher, C.R.: Development of and Flight Results From the Space Acceleration Measurement System (SAMS). NASA TM–105652 (AIAA Paper 92–0354), 1992.
8. DeLombard, R.; and Finley, B.D.: Space Acceleration Measurement System Description and Operations on the First Spacelab Life Sciences Mission. NASA TM–105301, 1991.
9. Rogers, M.J.B., et al.: Low Gravity Environment On-Board Columbia During STS–40. AIAA Paper 93–0833, 1993.
10. NASA Johnson Space Center: Shuttle Orbiter/Cargo Standard Interfaces Document. ICD 2-19001, fig. 3.1.1.4-1, 1991.
11. NASA Johnson Space Center: Shuttle Orbiter/Cargo Standard Interfaces Document. ICD 2-19001, fig. 3.1.1.1-1, 1991.
12. NASA Johnson Space Center: Attitude and Pointing Handbook. JSC-10511, rev. B, 1988.
13. Blanchard, R.C.; Nicholson, J.Y.; and Ritter, J.R.: Preliminary OARE Absolute Acceleration Measurements on STS–50. NASA TM–107724, 1993.

BIBLIOGRAPHY

Microgravity Environment

1. Rogers, M.J.B.; Matisak, B.P.; and Alexandar, J.I.D.: Venting Force Contributions—Quasi-Steady Acceleration on STS–50. Microgravity Science and Technology, vol. VII, no. 4, Feb. 1994, pp. 293–298.
2. Dunbar, B.J.; Thomas, D.A.; and Schoess, J.N.: The Microgravity Environment of the Space Shuttle Columbia Middeck During STS–32. NASA TP–3140, 1991.
3. Baugher, C.R.; Martin, G.L.; and DeLombard, R.: Review of the Shuttle Vibration Environment. AIAA Paper 93–0832, 1993.
4. Baugher, C.R.; Martin, G.L.; and DeLombard, R.: Low-Frequency Vibration Environment for Five Shuttle Missions. NASA TM–106059, 1993.
5. Rogers, M.J.B., et. al.: Low Gravity Environment On-Board Columbia During STS–40. AIAA Paper 93–0833, 1993.
6. Rogers, M.J.B., et. al.: A Comparison of Low-Gravity Measurements On-Board Columbia During STS–40. Microgravity Science and Technology, vol. VI, no. 3, Sept. 1993, pp. 207–216.
7. Blanchard, R.C.; Hinson, E.W.; and Nicholson, J.Y.: Shuttle High Resolution Accelerometer Package Experiment Results: Atmospheric Density Measurements Between 60 and 160 km. J. Spac. Rock., vol. 26, 1989, pp. 173–180.
8. Dunbar, B.J.; Giesecke, R.L.; and Thomas, D.A.: The Microgravity Environment of the Space Shuttle Columbia Payload Bay During STS–32. NASA TP–3141, 1991.

Mission Microgravity Environment Summary

1. Baugher, C.R.; and Henderson, F.H.: Early Summary Report of Mission Acceleration Measurements From STS–40. ACAP Project Report, Sept. 9, 1991.
2. Baugher, C.R.; and Henderson, F.H.: Early Summary Report of Mission Acceleration Measurements From STS–43. ACAP Project Report, March 2, 1992.
3. Baugher, C.R.; and Henderson, F.H.: Early Summary Report of Mission Acceleration Measurements From STS–42. ACAP Project Report, Aug. 7, 1992.
4. Baugher, C.R.; and Henderson, F.H.: Summary Report of Mission Acceleration Measurements From STS–47. ACAP Project Report, March 31, 1993.
5. Baugher, C.R.; and Henderson, F.H.: Summary Report of Mission Acceleration Measurements From STS–50. ACAP Project Report, Nov. 9, 1992.
6. Baugher, C.R.; and Henderson, F.H.: STS–52 Mission Acceleration Measurements Summary—Sensor Report. ACAP Project Report, Sept. 7, 1993.
7. Finley, B.D., Grodsinksy, C.; and DeLombard, R.: Summary Report of Mission Acceleration Measurements for Spacehab-01, STS–57. NASA TM–106514, 1994.
8. Rogers, M.J.B.; and DeLombard, R.: Summary Report of Mission Acceleration Measurements for STS–62. NASA TM–106773, 1994.
9. Rogers, M.J.B.; and DeLombard, R.: Summary Report of Mission Acceleration Measurements for STS–60, SPACEHAB-2. NASA TM–106797, 1994.
10. Rogers, M.J.B.; and DeLombard, R.: Summary Report of Mission Acceleration Measurements for STS–65. NASA TM–106871, 1995.
11. DeLombard, R.; and Rogers, M.J.B.: Quick Look Report of Acceleration Measurements on Mir Space Station During Mir-16. NASA TM–106835, 1995.
12. Rogers, M.J.B.; and DeLombard, R.: Summary Report of Mission Acceleration Measurements for STS–66. NASA TM–106914, 1995.

Instrumentation

1. Rogers, M.J.B.; Alexander, J.I.D.; and Snyder, R.: Analysis Techniques for Residual Acceleration Data NASA TM–103507, 1990.
2. Arrott, A.: Making Acceleration Data More Accessible and Useful to Microgravity Investigators. Presented at the 1988 TMS-AIME Annual Meeting (Phoenix, AZ), Jan. 1988.
3. Shyr, C.K.: COPS Transformation Algorithms for Ephemeris and Attitude Parameters. NASA GSFC 560–731.1, rev. 2, 1992.
4. Martin, G.L.; Baugher, C.R.; and DeLombard, R.: Vibration Environment: Acceleration Mapping Strategy and Microgravity Requirements for Spacelab and Space Station. IAF Paper 90–350, 1990.
5. DeLombard, R.: Proposed Ground-Based Control of Accelerometer on Space Station Freedom. NASA TM–105960, 1993.
6. DeLombard, R.; Finley, B. D.; and Baugher, C. R.: Development Of and Flight Results From the Space Acceleration Measurement System (SAMS). AIAA Paper 92–0354 (NASA TM–105652), 1992.
7. DeLombard, R.; and Finley, B. D.: Space Acceleration Measurement System Description and Operations on the First Spacelab Life Sciences Mission. NASA TM–105301, 1991.
8. DeLombard, R.: Early Mission Science Support: Space Acceleration Measurement System (SAMS). International Workshop on Vibration Isolation Technology for Microgravity Science Applications, NASA CP–10094, 1992.
9. Blanchard, R.C., et al.: Orbital Acceleration Research Experiment. J. Spac. Rock., vol. 24, 1986, pp. 504–511.
10. Cooke, M.P.: STS–60 Wake Shield Facility Payload Microgravity Measuring Device Quick-Look Report. JSC–26620, 1994.
11. Rogers, M.J.B.; Alexander, J.I.D.; and Schoess, J.: Detailed Analysis of Honeywell In-Space Accelerometer Data - STS-32—Crystal Microstructure Response to Different Types of Residual Acceleration. Microgravity Science and Technology, vol. VI, 1993, pp. 28–33.

Science Impacts

1. Alexander, J.I.D: Low-Gravity Experiment Sensitivity to Residual Acceleration: A Review. Microgravity Science and Technology, vol. 3, Sept. 1990, pp. 52–68.
2. de Groh III, H.C.; and Nelson, E.S.: On Residual Acceleration During Space Experiments. Heat Transfer in Microgravity Systems, S.S. Sadhal; and A. Gopinath, ed., HTD-Vol. 290, ASME, New York, 1994, pp. 23–33.
3. Favier, J.J., et al.: Mass Transport Phenomena During Solidification in Microgravity: Preliminary Results of the First MEPHISTO Flight Experiment. J Cryst. Growth, vol. 140, no. 1-2, June 1994, pp. 237–243.
4. Ramachandran, N.; and Winter, C.A.: Effects of g-jitter and Marangoni Convection on Float Zones. J Spac. Rock., vol. 29, no. 4, July-Aug. 1992, pp. 514–522.
5. Arnold, W.A., et al.: Three-Dimensional Flow Transport Modes in Directional Solidification During Space Processing. J. Spac. Rock., vol. 28, Mar–Apr. 1991, pp. 238–243.
6. Nelson, E.S.: An Examination of Anticipated g-jitter on Space Station and Its Effects on Materials Processes. NASA TM–103775, 1994.

REPORT DOCUMENTATION PAGE

Form Approved
OMB No. 0704-0188

1. AGENCY USE ONLY (*Leave blank*)	2. REPORT DATE	3. REPORT TYPE AND DATES COVERED
	August 1996	Technical Memorandum

4. TITLE AND SUBTITLE

Compendium of Information for Interpreting the Microgravity Environment of the Orbiter Spacecraft

5. FUNDING NUMBERS

WU–963–60–0D

6. AUTHOR(S)

Richard DeLombard

7. PERFORMING ORGANIZATION NAME(S) AND ADDRESS(ES)

National Aeronautics and Space Administration
Lewis Research Center
Cleveland, Ohio 44135–3191

8. PERFORMING ORGANIZATION REPORT NUMBER

E–9851

9. SPONSORING/MONITORING AGENCY NAME(S) AND ADDRESS(ES)

National Aeronautics and Space Administration
Washington, D.C. 20546–0001

10. SPONSORING/MONITORING AGENCY REPORT NUMBER

NASA TM–107032

11. SUPPLEMENTARY NOTES

Responsible person, Richard DeLombard, organization code 6743, (216) 433–5285.

12a. DISTRIBUTION/AVAILABILITY STATEMENT

Unclassified - Unlimited
Subject Categories 20, 35, and 18

This publication is available from the NASA Center for Aerospace Information, (301) 621–0390.

12b. DISTRIBUTION CODE

13. ABSTRACT ***(Maximum 200 words)***

Science experiments are routinely conducted on the NASA shuttle Orbiter vehicles. Primarily, these experiments are operated on such missions to take advantage of the microgravity (low-level acceleration) environment conditions during on-orbit operations. Supporting accelerometer instruments are operated with the experiments to measure the microgravity acceleration environment in which the science experiments were operated. The Principal Investigator Microgravity Services (PIMS) Project at NASA Lewis Research Center interprets these microgravity acceleration data and prepares mission summary reports to aid the principal investigators of the scientific experiments in understanding the microgravity environment. Much of the information about the Orbiter vehicle and the microgravity environment remains the same for each mission. Rather than repeat that information in each mission summary report, reference information is presented in this report to assist users in understanding the microgravity-acceleration data. The characteristics of the microgravity acceleration environment are first presented. The methods of measurement and common instruments used on Orbiter missions are described. The coordinate systems utilized in the Orbiter and accelerometers are described. Some of the Orbiter attitudes utilized in microgravity related missions are illustrated. Methods of data processing are described and illustrated. The interpretation of the microgravity acceleration data is included with an explanation of common disturbance sources. Instructions to access some of the acceleration data and a description of the Orbiter thrusters are explained in the appendixes. A microgravity environment bibliography is also included.

14. SUBJECT TERMS

Microgravity environment; Acceleration; Orbiter; Acceleration analysis; Microgravity disturbances

15. NUMBER OF PAGES

44

16. PRICE CODE

A03

17. SECURITY CLASSIFICATION OF REPORT	18. SECURITY CLASSIFICATION OF THIS PAGE	19. SECURITY CLASSIFICATION OF ABSTRACT	20. LIMITATION OF ABSTRACT
Unclassified	Unclassified	Unclassified	